Friction forces on phase transition fronts

Ariel Mégevand*
IFIMAR (CONICET-UNMdP),
Departamento de Física, Facultad de Ciencias Exactas y Naturales, UNMdP,
Deán Funes 3350, (7600) Mar del Plata, Argentina

Abstract

In cosmological first-order phase transitions, the microscopic interaction of the phase transition fronts with non-equilibrium plasma particles manifests itself macroscopically as friction forces. In general, it is a nontrivial problem to compute these forces, and only two limits have been studied, namely, that of very slow walls and, more recently, ultra-relativistic walls which run away. In this paper we consider ultra-relativistic velocities and show that stationary solutions still exist when the parameters allow the existence of runaway walls. Hence, we discuss the necessary and sufficient conditions for the fronts to actually run away. We also propose a phenomenological model for the friction, which interpolates between the non-relativistic and ultra-relativistic values. Thus, the friction depends on two friction coefficients which can be calculated for specific models. We then study the velocity of phase transition fronts as a function of the friction parameters, the thermodynamic parameters, and the amount of supercooling.

1 Introduction

Cosmological phase transitions may have observable consequences. In particular, first-order phase transitions provide a departure from thermal equilibrium, which may give rise to a variety of cosmological relics, such as the baryon asymmetry of the universe [1], cosmic magnetic fields [2], topological defects [3], baryon inhomogeneities [4, 5], and gravitational waves [6]. In a first-order phase transition, bubbles of the stable phase nucleate and grow inside the supercooled phase. The velocity of the phase transition fronts (bubble walls) is an important parameter for the generation of cosmological relics. For instance, generating sizeable gravitational waves requires high velocities, whereas the generation of baryon number in the electroweak phase transition peaks at small velocities.

The wall velocity is governed in principle by the pressure difference between the two phases. However, the wall propagation disturbs the plasma, and the latter resists the

*Member of CONICET, Argentina. E-mail address: megevand@mdp.edu.ar

motion of the wall. This opposition manifests itself in two ways. Microscopically, the interactions of non-equilibrium plasma particles with the wall cause a friction force on the latter [7, 8, 9, 10]. Besides, the latent heat that is released at the phase transition fronts causes temperature variations in the plasma [11, 12, 13, 14], which tend to diminish the pressure difference between phases. These two mechanisms are called microphysics and hydrodynamics, respectively.

Microphysics is a very difficult subject and for several years was considered only in the non-relativistic (NR) limit. As a consequence, phenomenological models have been used in order to extrapolate the friction force to higher velocities. The general approach is based on adding a covariant damping term $\eta u^\mu \partial_\mu \phi$ to the field equation, where u^μ is the four-velocity of the plasma (see, e.g., [5, 12]). This gives a friction force of the form $F_{\rm fr} \sim \eta \gamma_w v_w$, where v_w is the wall velocity and $\gamma_w = 1/\sqrt{1-v_w^2}$. The parameter η can be determined by considering the limit $v_w \to 0$ and comparing with microphysics calculations.

Recently, the opposite limit was considered [10]. The total force acting on the electroweak bubble wall was derived for an ultra-relativistic (UR) wall propagating with extremely large values of the gamma factor. For such a fast moving wall the physics is quite simpler than in the NR case, since the plasma is almost unaffected by the passage of the wall. The resulting total force does not depend on the wall velocity. As a consequence, if the force is positive, then the wall runs away (i.e., as the wall propagates, γ_w grows linearly with the propagation distance). If the total force turns out to be negative, then the initial assumption of an extremely ultra-relativistic wall is incorrect and the wall must reach a slower, stationary state. Thus, we have a simple criterion for the existence of runaway solutions. The results of Ref. [10] motivated modifications to the usual phenomenological models for the friction, so that the friction saturates for large γ_w [15, 16]. The modifications essentially amount to eliminating the gamma factor from the friction force, so that $F_{\rm fr} \sim \eta v_w$.

We wish to point out that the runaway condition found in Ref. [10] is only a necessary condition for the existence of the runaway solution. It does not guarantee that the runaway solution will actually be realized. Indeed, it is well known that different propagation modes can exist for the same set of parameters (due to nonlinear hydrodynamics). Therefore, the runaway solution may coexist with a stationary solution (a detonation or a deflagration). Moreover, before any ultra-relativistic behavior is important, a bubble wall first needs to be accelerated to an ultra-relativistic velocity. Whether that is possible or not, always depends on non-relativistic physics. Suppose a stationary solution with a certain velocity $v_w = v_0$ exists. At some point during acceleration, the wall velocity will take that value. One expects that, provided the stationary solution is stable, the wall will stay in that state instead of continuing accelerating[1]. Deflagration solutions can be hydrodynamically unstable, but detonations are stable [17]. Hence, the wall will probably not run away whenever it can propagate as a detonation.

[1]It may happen, however, that, as the wall velocity reaches the value v_0, the hydrodynamical configuration (i.e., the fluid velocity and temperature profile) does not match the corresponding stationary solution, and the wall does not stay in that state (see, e.g., [14]).

We also notice that a single-parameter phenomenological model of the form $F_{\rm fr} = \eta v_w$ will hardly give the correct values of the friction force in both ultra-relativistic and non-relativistic limits. In particular, the parameter η should be obtained from microphysics calculations in either limit.

The main goals of this paper are the following. In the first place, we wish to identify the friction force in the UR limit, in order to treat very fast but stationary solutions. This can be done by decomposing the total force obtained in Ref. [10] into a driving force and a friction force. Notice, though, that it is not clear in principle which is the correct decomposition, since there is no velocity-dependent term in this force. Furthermore, hydrodynamics is different in the stationary and runaway regimes. Secondly, we wish to consider the existence of stationary and runaway solutions and discuss the necessary and sufficient conditions for the wall to run away. In the third place, we wish to construct a well-motivated phenomenological model, which interpolates between the NR and UR limits. The model will have two free parameters (computable from microphysics) and will allow us to treat stationary solutions with intermediate velocities. We also wish to discuss the case of phase transitions with a large amount of supercooling, which favor fast-moving phase transition fronts.

The plan is the following. In section 2 we briefly review the dynamics of cosmological phase transitions and the hydrodynamic solutions for stationary fronts. In section 3 we discuss the friction forces. We introduce an ultra-relativistic friction parameter and we discuss the conditions for the wall to run away. In section 4 we discuss a phenomenological model for the friction. In section 5 we consider the bag equation of state to obtain analytical formulas for the wall velocity and for the runaway conditions. We also analyze the general dependence of the bubble wall velocity on the friction and thermodynamic parameters. Finally, in section 6 we discuss the case of strong supercooling. We summarize our results in section 7.

2 Phase transition dynamics

A cosmological phase transition is described in general by a scalar field ϕ which acts as an order parameter. We shall consider the case in which ϕ is a Higgs field. The finite temperature behavior of the system is determined by the free energy density (finite-temperature effective potential)

$$\mathcal{F}(\phi, T) = V(\phi) + V_T(\phi), \tag{1}$$

where $V(\phi)$ is the zero-temperature effective potential and $V_T(\phi)$ the finite-temperature correction. To one-loop order, the latter is given by [18]

$$V_T(\phi) = \sum_i \pm g_i T \int \frac{d^3p}{(2\pi)^3} \log\left(1 \mp e^{-E_i/T}\right). \tag{2}$$

where the sum runs over particle species, g_i is the number of degrees of freedom of species i, the upper sign stands for bosons, the lower sign stands for fermions, and

$E_i = \sqrt{p^2 + m_i^2(\phi)}$. Here, m_i are the field-dependent masses. There is also a correction from the resummed daisy diagrams for bosons. For our discussions it is not necessary to consider the exact form of this correction. Its effect is to modify the cubic term in the expansion of V_T in powers of m_i/T, as we shall comment below.

In thermal equilibrium, the field lies at a minimum of the free energy. If there are several minima, then different phases are possible for the system, and phase transitions may occur. In the simplest case we have a high-temperature minimum $\phi_+(T)$ (in general, $\phi_+ \equiv 0$) and a low-temperature one $\phi_-(T)$. For a first-order phase transition, these two minima coexist in a certain range of temperatures, separated by a barrier. All the properties of a given phase are derived from $\mathcal{F}$, once it is evaluated at a minimum. Thus, the two phases are characterized by the free energy densities

$$\mathcal{F}_+(T) \equiv \mathcal{F}(\phi_+(T), T), \quad \mathcal{F}_-(T) \equiv \mathcal{F}(\phi_-(T), T), \tag{3}$$

which give different equations of state (EOS). The energy density is given by $\rho_\pm(T) = \mathcal{F}_\pm(T) - T\mathcal{F}'_\pm(T)$, where a prime indicates a derivative with respect to T. The pressure is given by $p_\pm(T) = -\mathcal{F}_\pm(T)$. The enthalpy density is given by $w_\pm = \rho_\pm + p_\pm$, and the entropy density by $s_\pm = w_\pm/T$. The speed of sound is given by $c_\pm^2(T) = \partial p_\pm/\partial\rho_\pm = p'_\pm(T)/\rho'_\pm(T)$. The phases are in equilibrium at the critical temperature T_c, defined by $\mathcal{F}_+(T_c) = \mathcal{F}_-(T_c)$. The energy density difference at $T = T_c$ is called the latent heat $L \equiv \rho_+(T_c) - \rho_-(T_c)$.

The phase transition occurs, in principle, when the Universe reaches the critical temperature. However, the nucleation rate vanishes at $T = T_c$. Bubbles of the stable phase effectively begin to nucleate at a temperature T_n below T_c [19]. The nucleated bubbles expand due to the pressure difference between the two phases (at $T < T_c$). The phase transition fronts move with a velocity v_w which depends on the pressure difference and the friction with the surrounding plasma. The release of latent heat causes local reheating and bulk motions of the plasma. Considering the development of a phase transition involves solving a set of coupled equations for several quantities, each of which is not easy to compute, such as the nucleation rate, the wall velocity, and the temperature. The latter varies due to the expansion of the universe and the release of energy at the phase transition (for the dynamics of phase transitions see, e.g., [20]). Here we shall concentrate on the motion of phase transition fronts for a given nucleation temperature T_n.

Thus, the relevant variables are the scalar field $\phi(\mathbf{x}, t)$, the temperature $T(\mathbf{x}, t)$, and the velocity $v(\mathbf{x}, t)$ of the plasma. We shall consider the thin-wall approximation for the field profile. Thus, we shall assume that the field varies in an infinitely thin region, outside which ϕ is a constant. For the macroscopic treatment this is a good approximation, since the wall width is much smaller than the width of the fluid profiles [21]. We shall consider planar-symmetry fronts moving in the z direction (see [22] for a discussion on considering different wall geometries). As a consequence of the friction with the plasma, the bubble wall often reaches a terminal velocity in a very short time after bubble nucleation. In the rest of this section we shall review the hydrodynamics for stationary phase transition fronts.

2.1 Hydrodynamics for stationary fronts

The equations for the fluid variables can be obtained from the conservation of the energy-momentum tensor, $\partial_\mu T^{\mu\nu} = 0$. For stationary profiles moving at constant velocity, it is useful to consider the rest frame of the front. The relation between the fluid variables on each side of the wall is well known [23],

$$w_- v_- \gamma_-^2 = w_+ v_+ \gamma_+^2, \tag{4}$$

$$w_- v_-^2 \gamma_-^2 + p_- = w_+ v_+^2 \gamma_+^2 + p_+, \tag{5}$$

where $\gamma_\pm = 1/\sqrt{1 - v_\pm^2}$, and we have used a + sign for variables in front of the wall and a − sign for variables behind the wall (which correspond to the + and − phases, respectively). For an infinitely thin interface, Eqs. (4-5) determine the discontinuity of the fluid profiles at the phase transition front. There can also be discontinuities in the fluid profiles away from the bubble wall. These are called *shock fronts*. In such surfaces, the temperature and fluid velocity are discontinuous but the EOS is the same on both sides. In the reference frame of shock fronts Eqs. (4-5) still apply.

Since there is no characteristic distance scale in the fluid equations, it is usual to assume the *similarity condition* [23], namely, that w, p and v depend only on $\xi = z/t$. In the planar-symmetry case we have either constant solutions $v(\xi) =$ constant, or a "rarefaction wave" solution $v_{\rm rar}(\xi) = (\xi - c)/(1 - \xi c)$, where c is the speed of sound (see, e.g., [22, 21] for recent discussions). The fluid velocity profile is constructed from these solutions, using the matching conditions (4-5) and appropriate boundary conditions.

For a given set of thermodynamical parameters, Eqs. (4) and (5) give v_+ as a function of v_-. The solutions have two branches, called *detonations* and *deflagrations* (see, e.g., [24]). For detonations the incoming flow is faster than the outgoing flow ($|v_+| > |v_-|$) and is supersonic ($|v_+| > c_+$) for any value of v_- in the range $-1 < v_- < 0$. For deflagrations, we have $|v_+| < |v_-|$ and $|v_+| < c_+$. At $|v_-| = c_-$, the value of $|v_+|$ is a minimum for detonations and a maximum for deflagrations. At this point the hydrodynamic process is called a *Jouguet* detonation or deflagration. We denote the corresponding values by $|v_+| = v_J^{\rm det}$ and $|v_+| = v_J^{\rm def}$, respectively. The hydrodynamic process is called *weak* if the velocities v_+ and v_- are either both supersonic or both subsonic. Otherwise, the hydrodynamic process is called *strong*.

The fluid temperature and velocity profiles depend on the boundary conditions far behind the wall (at the center of the bubble) and far in front of the wall, where information on the bubble has not arrived yet. Thus, the fluid velocity vanishes far behind and far in front of the wall. Furthermore, the temperature far in front of the wall is given by the temperature T_n at which the bubble nucleated. Three kinds of solutions are compatible with these requirements: a weak detonation, for which the wall is supersonic, a Jouguet deflagration, which is also supersonic, and a weak deflagration, which is subsonic.

The relevant properties of these solutions are the following (see, e.g., [21, 22] for details). For the supersonic detonation, the fluid in front of the wall is unperturbed and we have $v_w = -v_+, T_+ = T_n$. Hence, we have $v_w \geq v_J^{\rm det}$. The fluid profile behind the wall is given by the rarefaction wave. The strong detonation solution must be discarded

because it is not possible to construct a fluid profile for it. For the deflagration, the fluid velocity in front of the wall is not at rest, and there is a supersonic shock front preceding the wall. Beyond the shock, the fluid is still unperturbed at temperature T_n. The solution between the phase-transition and shock fronts is a constant. The boundary condition for deflagrations is often considered to be that the fluid behind the wall is at rest. In this case, we have $v_w = -v_-$. This "traditional" deflagration can be either weak (and subsonic), or strong (and supersonic). The limit between these solutions is a Jouguet deflagration with $v_w = c_-$. It has been argued that strong deflagrations are unstable[2] and should not be considered [12, 13, 14]. However, supersonic deflagrations that are not strong can exist [13] if we relax the boundary condition that the fluid is at rest behind the wall. Thus, if the condition $v_- = -v_w$ is replaced by $v_- = -c_-$, we have a Jouguet deflagration with $|v_+| = v_J^{\rm def} < c_+$. In this case the wall is followed by a rarefaction wave. Since the wall moves at the speed of sound with respect to the fluid behind it, and the fluid also moves with respect to the center of the bubble, the wall velocity is supersonic. This solution fills the velocity gap between the weak deflagration and the detonation, $c_- \leq v_w \leq v_J^{\rm det}$.

3 Microphysics

The forces acting on the bubble wall can be derived from the equation of motion for the background field ϕ. It is usual to consider the WKB approximation, which makes sense if the scale of variation of ϕ is not too short. We have [7]

$$\partial_\mu \partial^\mu \phi + \frac{\partial V}{\partial \phi} + \sum_i g_i \frac{dm_i^2}{d\phi} \int \frac{d^3p}{(2\pi)^3 2E_i} f_i(p,x) = 0, \tag{6}$$

where f_i is the distribution function of particle species i. In general, a distribution function can be written as

$$f_i(p) = f_i^{\rm eq}(p) + \delta f_i(p,x), \tag{7}$$

where $f_i^{\rm eq}(p) = 1/(e^{E_i/T} \mp 1)$ is the equilibrium distribution function and δf_i is a deviation. Inserting this decomposition into Eq. (6), the term $f_i^{\rm eq}$ just gives $\partial V_T/\partial\phi$ (i.e., the finite-temperature corrections to the effective potential) and we obtain

$$\partial_\mu \partial^\mu \phi + \frac{\partial \mathcal{F}}{\partial \phi} + \sum_i g_i \frac{dm_i^2}{d\phi} \int \frac{d^3p}{(2\pi)^3 2E_i} \delta f_i = 0. \tag{8}$$

We shall assume for simplicity that the phase transition occurs from a vanishing minimum to a non-vanishing one, as in the usual symmetry braking case. We shall denote ϕ_0 the non-vanishing minimum, i.e.,

$$\phi_+(T) \equiv 0, \quad \phi_-(T) \equiv \phi_0(T) \tag{9}$$

An equation for the bubble wall can be obtained if we assume a fixed field profile centered at the wall position $z_w(t)$. Thus, consider the dependence $\phi(z,t) = \phi[\gamma_w(z - z_w)]$.

[2] Even weak deflagrations may be unstable [17].

The exact form of the one-variable function $\phi(z)$ is not relevant. It is often assumed to be given by a tanh. It varies from the value $\phi(-\infty) = \phi_0$ (inside the bubble) to $\phi(+\infty) = 0$ (outside the bubble). The variation occurs in a small region of width l_w (the bubble wall). In the reference frame which instantaneously moves with the wall, in which $z_w = 0$ and $\dot{z}_w = 0$, we have $\gamma_w = 1, \dot{\gamma}_w = 0$ and $\ddot{\gamma}_w = \ddot{z}_w^2$, where a dot indicates a derivative with respect to t. The first term in Eq. (8) gives $(\ddot{z}_w^2 z - \ddot{z}_w)\phi'(z) - \phi''(z)$, where a prime indicates a total derivative with respect to z. Notice that the function $\phi'(z)$ has a peak inside the wall and vanishes outside. We can define the wall position so that $\int z\phi'^2 dz = 0$. Then, if we multiply Eq. (8) by ϕ' and integrate across the wall, we obtain

$$\sigma \ddot{z}_w = F_{\rm dr}/A + F_{\rm fr}/A, \tag{10}$$

where $\sigma \equiv \int \phi'^2 dz$ is the surface tension, and

$$\frac{F_{\rm dr}}{A} = \int \frac{\partial \mathcal{F}(\phi, T)}{\partial \phi} \frac{d\phi}{dz} dz, \tag{11}$$

$$\frac{F_{\rm fr}}{A} = \sum_i g_i \int dz \frac{dm_i^2}{dz} \int \frac{d^3p}{(2\pi)^3 2E_i} \delta f_i \tag{12}$$

are the forces per unit area acting on the wall.

The force $F_{\rm fr}$ depends on the interactions of the plasma particles with the wall and may be regarded as a friction force. Indeed, for small wall velocity v_w (in the reference frame of the bubble center), this force turns out to be proportional to v_w. As a consequence, the wall may reach a terminal velocity. The force $F_{\rm dr}$ does not depend on microphysics details, and may be regarded as the driving force.

3.1 The driving force

To see the behavior of this force, let us consider a wall which moves very slowly, so that equilibrium can be assumed and $F_{\rm fr}$ vanishes in Eq. (10). For such a slow wall, the temperature will be homogeneous, $T(z) =$ constant. Hence, the integral in Eq. (11) yields $\mathcal{F}(\phi_+, T) - \mathcal{F}(\phi_-, T)$. Thus, we obtain the equation $\sigma \ddot{z}_w = p_-(T) - p_+(T)$, which is positive for $T < T_c$. Therefore, if the wall is initially moving very slowly, it will accelerate due to the pressure difference. As a consequence, the wall motion will cause departures from local equilibrium and a friction force will appear. Besides, inhomogeneous reheating will arise, which affects the driving force.

For the integral in Eq. (11) we may use the identity $(\partial \mathcal{F}/\partial \phi)(d\phi/dz) = d\mathcal{F}/dz - (\partial \mathcal{F}/\partial T)(dT/dz)$ [12, 26], so that the driving force can be expressed as

$$\frac{F_{\rm dr}}{A} = p_-(T_-) - p_+(T_+) + \int_{T_-}^{T_+} s(\phi, T) dT, \tag{13}$$

where the entropy density is given by $s = -\partial \mathcal{F}/\partial T$. In order to obtain analytical results, in this paper we shall use approximations for integrals across the wall. Our aim is to

obtain expressions which only depend on variables defined outside the wall, namely, the values of $v_\pm$, $T_\pm$, etc., which can be obtained using Eqs. (4-5), the EOS, and appropriate boundary conditions. For the integral in Eq. (13), we shall approximate the entropy density by the average value $\langle s \rangle = (s_+ + s_-)/2$. This gives the approximation [26]

$$\frac{F_{\rm dr}}{A} = p_-(T_-) - p_+(T_+) + \langle s \rangle \, (T_+ - T_-) \, . \tag{14}$$

If we neglect hydrodynamics and consider a homogeneous temperature, we obtain the pressure difference $p_-(T) - p_+(T)$. This is very sensitive to the departure of T from T_c. Besides, $p_-(T_-) - p_+(T_+)$ is very sensitive to the difference $T_+ - T_-$. Indeed, the pressure difference may be positive or negative depending on the value of $T_+ - T_-$. The general effect of hydrodynamics is to slow down the wall [26, 27].

3.2 Friction force

The friction force $F_{\rm fr}$ is in general much more difficult to calculate than $F_{\rm dr}$. It has been extensively studied for small wall velocities [7, 8], since temperature gradients can be neglected and the deviations from equilibrium can be assumed to be small. Even in this case, computing the deviations δf_i involves solving a complex system of Boltzmann equations. Recently [10], the total force acting on the bubble wall was derived for a wall which propagates ultra-relativistically. The treatment turns out to be quite simpler.

3.2.1 Non-relativistic limit

For small velocities we have $\delta f_i \propto v_w$, and Eq. (12) gives a friction term of the form

$$\frac{F_{\rm fr}}{A} = -\eta_{\rm NR} v_w . \tag{15}$$

The non-relativistic friction coefficient $\eta_{\rm NR}$ depends on the couplings of the particles to the Higgs, and also on the interactions of plasma particles, which tend to restore the equilibrium. Effective interaction rates $\Gamma_{ij} \sim T$ appear in the equations for δf_i, coming from the collision integral in the Boltzmann equation. The "thick wall" limit $\Gamma \gg 1/l_w$ is often used, which leads to analytical results (see, e.g., [8]). Here we shall use the results from the simplified treatment of Refs. [25, 28]. For masses of the form $m_i^2 = h_i^2 \phi^2 + \mu_i^2$ we have

$$\eta_{\rm NR} \approx \sum_i \frac{g_i h_i^4}{\Gamma} \int_{-\infty}^{+\infty} c_{1i}^2(\phi) \, \phi^2 \phi'^2 dz . \tag{16}$$

where Γ is an average interaction rate (typically, $\Gamma \lesssim 10^{-1} T$), and the function $c_1(\phi)$ is given by

$$c_1 \equiv \frac{1}{T^2} \int \frac{d^3p}{(2\pi)^3 \, E} \frac{e^{E/T}}{(e^{E/T} \mp 1)^2} . \tag{17}$$

Notice the strong dependence of the coefficient c_1 on the ratio m/T. Different limiting cases have been analyzed in Ref. [28]. For a "typical" phase transition with $\phi \sim T \sim T_c$,

one can often use an expansion in powers of m/T. To lowest order, we have $c_1 = \log\chi/2\pi^2$, where $\chi = 2$ for fermions and $\chi = T/m$ for bosons. Hence, in this case the dependence on ϕ is at most logarithmic, and we can regard c_1 as a constant for the integral in (16). We obtain

$$\eta_{\rm NR} = \frac{\hat{\eta}_{\rm NR}}{T}\int \phi^2\phi'^2 dz, \tag{18}$$

where

$$\hat{\eta}_{\rm NR} \equiv \sum_i \frac{g_i h_i^4}{\Gamma/T}\left(\frac{\log\chi_i}{2\pi^2}\right)^2 \tag{19}$$

The dimensionless coefficient $\hat{\eta}_{\rm NR}$ depends on details of the model, whereas the integral in Eq. (18) depends only on the wall shape. This integral can be estimated as $\int \phi^2\phi'^2 dz \sim \phi_0^2\sigma \sim \phi_0^4/l_w$, where l_w is the wall width. Typically, $l_w \gtrsim T^{-1}$. These rough approximations give in principle the correct parametric behavior, but omit numerical factors which may be as high as ~ 10. To obtain quantitatively useful values, we may "calibrate" the friction with a known model [16, 29]. In our approximation (19), this can be accomplished by choosing a suitable value of Γ/T. For instance, considering the top, Z and W contributions to (19), we obtain the correct SM values ($\hat{\eta}_{\rm NR} \approx 0.6$ [16]) if we use $\Gamma \sim 10^{-2}T$.

3.2.2 Ultra-relativistic limit

For a wall which has reached ultra-relativistic velocities with very large gamma factor, several approximations are justified [10]. In the frame of the wall, plasma particles always have enough energy to surpass the wall, and the reflection coefficients are exponentially suppressed. Incoming particles have received no signal that the wall is approaching and are in equilibrium. Besides, interactions between plasma particles are time delayed and can be neglected. Thus, the occupancies evolve undisturbed. As a consequence, only the equilibrium occupancies of the symmetric phase are needed in the calculation. To lowest order in $1/\gamma_w$, the net force per unit area acting on the wall is given by [10]

$$\frac{F}{A} = V(\phi_+) - V(\phi_-) - \sum_i g_i[m_i^2(\phi_-) - m_i^2(\phi_+)]\int \frac{d^3p}{(2\pi)^3 2E_{i+}} f_{i+}^{\rm eq}(p). \tag{20}$$

This force does not depend on the wall velocity. Therefore, if it is positive the wall will accelerate indefinitely. On the other hand, if F/A is negative, then the wall in fact cannot reach the ultra-relativistic regime.

Notice that the result (20) can be obtained directly from Eq. (6), by evaluating the momentum integral in the + phase. Thus, it does not require the decomposition into equilibrium occupancies and deviations. We are interested in such a decomposition, though. More precisely, we intend to decompose the total force into a driving force and a friction force. This will help us to introduce, in the next section, a phenomenological model for the friction which interpolates between the non-relativistic and the ultra-relativistic

limits. Adding and subtracting in Eq. (20) the finite-temperature correction $V_{T_+}(\phi_+)$ for the + phase, we have

$$\frac{F}{A} = \mathcal{F}(\phi_+, T_+) - \tilde{\mathcal{F}}(\phi_-, T_+), \tag{21}$$

where $\tilde{\mathcal{F}}(\phi_-, T_+)$ is the mean field effective potential, obtained by keeping only the quadratic terms in a Taylor expansion of V_T about the + phase [10, 15],

$$\tilde{\mathcal{F}}(\phi_-, T_+) = V(\phi_-) + V_{T_+}(\phi_+) + \sum_i [m_i^2(\phi_-) - m_i^2(\phi_+)] \left.\frac{dV_T}{dm_i^2}\right|_+ . \tag{22}$$

In contrast to the non-relativistic case, the total force in (21) does not have a velocity-dependent term, which could be identified as a friction force. Nevertheless, we can still decompose the force into a part which comes from the equilibrium distributions (the driving force) and a part coming from the deviations (the friction force). The particles in front of the wall are in equilibrium at temperature T_+ and pressure $p_+(T_+) = -\mathcal{F}(\phi_+, T_+)$. The departures from equilibrium occur at the wall and behind. The corresponding friction force must come from the term $-\tilde{\mathcal{F}}(\phi_-, T_+)$ in Eq. (21). We only need to isolate the equilibrium part.

The problem with such a decomposition is that it is not clear which would be the temperature behind the wall. In the stationary case the temperature T_- can be calculated from Eqs. (4-5) and is different from T_+. In the limit $v_w \to 1$ (i.e., for a very fast detonation) we still obtain $T_- \neq T_+$. Nevertheless, there is no reason to assume that the stationary solution should match the runaway solution. Notice that the only temperature appearing in Eqs. (21-22) is T_+, suggesting that, in the runaway case, we have $T_- = T_+$. Indeed, for stationary solutions the released latent heat goes into bulk motions of the fluid and reheating of the plasma, whereas for runaway solutions the energy goes mainly into accelerating the wall. Assuming $T_- = T_+$, the occupancies in each phase (in the plasma frame) are given by

$$f_{i+}(p_+) = 1/[\exp(E_{i+}/T_+) \mp 1], \tag{23}$$

$$f_{i-}(p_-) = 1/[\exp(E_{i-}/T_+) \mp 1] + \delta f_i, \tag{24}$$

with $E_{i\pm}^2 = p_\pm^2 + m_{i\pm}^2$.

In fact, we can calculate the exact form of the occupancies just behind the wall. After the passage of the wall the occupancies $f_{i+}(p_+)$ are undisturbed, but the energy and momentum of a particle have changed. In the plasma frame, these changes are given by [10]

$$E_{i-} - E_{i+} = p_- - p_+ = \frac{m_{i-}^2 - m_{i+}^2}{2(E_{i-} - p_-)}. \tag{25}$$

We thus have $E_{i+}(p_+) = E_{i-}(p_-) + (m_{i+}^2 - m_{i-}^2)/[2(E_{i-} - p_-)]$, and

$$f_{i-}(p_-) = \left[\exp\left(\frac{E_{i-}(p_-)}{T_+} + \frac{m_{i+}^2 - m_{i-}^2}{2(E_{i-} - p_-)T_+}\right) \mp 1\right]^{-1} . \tag{26}$$

It seems natural to decompose the occupancies (26) in the form (24), which can be taken as the definition of δf_i. If, e.g., the mass difference $m_{i+} - m_{i-}$ is small, then the deviation δf_i will be small too.

According to Eqs. (24) and (26), the deviations from equilibrium vanish only in front of the bubble wall, in contrast with the non-relativistic case, in which the deviations vanish also behind the wall. Indeed, the $(\phi')^2$ factor in Eq. (16) indicates that the deviations are localized at the bubble wall. The difference arises because, in the UR case, the wall has passed so quickly that there was no time for the plasma to recover the equilibrium. Notice, anyway, that Eq. (26) gives the occupancies behind the wall but close to it. At some distance behind the wall the plasma will reach the equilibrium (and some reheating will occur).

It is easy to obtain the macroscopic version of the decomposition (24), directly from Eq. (21). For $T_- = T_+$, the driving force is given by

$$\frac{F_{\rm dr}}{A} = \mathcal{F}(\phi_+, T_+) - \mathcal{F}(\phi_-, T_+). \tag{27}$$

Therefore, the departure from equilibrium causes a friction force given by

$$\frac{F_{\rm fr}}{A} = \mathcal{F}(\phi_-, T_+) - \tilde{\mathcal{F}}(\phi_-, T_+), \tag{28}$$

Since $v_w \simeq 1$, we can define an ultra-relativistic friction coefficient $\eta_{\rm UR}$ by

$$\eta_{\rm UR} = -F_{\rm fr}/A, \tag{29}$$

so that the total force is given by

$$\frac{F}{A} = (p_- - p_+)|_{T_+} - \eta_{\rm UR} v_w. \tag{30}$$

Notice that we may also write Eq. (21) as $F/A = \tilde{\mathcal{F}}(\phi_+, T_+) - \tilde{\mathcal{F}}(\phi_-, T_+)$, since $\tilde{\mathcal{F}}(\phi_+, T_+) = \mathcal{F}(\phi_+, T_+)$. If this mean-field potential difference is negative, then the bubble wall cannot run away. For instance, the wall never runs away in a "fluctuation induced" first-order phase transition [10], i.e., a phase transition which is first-order due to the thermal part of the effective potential, V_T. For example, consider the well known high-temperature expansion of Eq. (2),

$$V_T(\phi) = -\sum_i \frac{\pi^2 g_i c_i' T^4}{90} + \sum_i g_i c_i \frac{T^2 m_i^2(\phi)}{24} - \sum_{\rm bosons} g_i \frac{T m_i^3(\phi)}{12\pi} + \mathcal{O}(m^4), \tag{31}$$

which is valid for many models. Here, $c_i = 1$ (1/2) and $c_i' = 1$ (7/8) for bosons (fermions). Only bosons contribute to the m_i^3 terms. In fact, after the resummation of daisy diagrams, only the transverse polarizations of gauge bosons remain in general in this contribution. The cubic term in Eq. (31) is very important since it may cause a barrier in the free energy and, thus, a first-order phase transition. This term is not present in the mean field

potential. If the first-order character of the phase transition is due to this term alone, then in the mean field potential the minimum ϕ_- will raise above the minimum ϕ_+. As a consequence, the net force (21) will be negative and the wall will reach a terminal velocity.

Let us consider the friction coefficient $\eta_{\rm UR}$ for the case $m/T \ll 1$ (as we did for $\eta_{\rm NR}$). According to Eq. (31) we have, to lowest order in m/T,

$$\eta_{\rm UR} \approx \sum_{\rm bosons} \frac{g_i T}{12\pi} \left[m_i^3(\phi_-) - m_i^3(\phi_+) \right] . \tag{32}$$

We have assumed that the contribution of gauge bosons is important. Otherwise, the $\mathcal{O}(m^4)$ terms should be considered. The generalization is straightforward. Let us further simplify the problem by specifying to the case $\phi_+ = 0$ and assuming particle masses of the form $m_i(\phi) = h_i \phi$. Then, we have

$$\eta_{\rm UR} \approx \sum_{\rm bosons} \frac{g_i h_i^3}{12\pi} T \phi_0^3 \equiv \hat{\eta}_{\rm UR} T \phi_0^3, \tag{33}$$

where we used again the notation ϕ_0 for the symmetry-braking minimum, and we have defined a dimensionless coefficient $\hat{\eta}_{\rm UR}$ which contains the parameters of the model.

3.3 Runaway conditions

According to Eqs. (10) and (30), in the runaway regime we have

$$\sigma \ddot{z}_w = p_-(T_+) - p_+(T_+) - \eta_{\rm UR}, \tag{34}$$

which gives the necessary condition for the wall to run away,

$$p_-(T_+) - p_+(T_+) > \eta_{\rm UR}. \tag{35}$$

This condition does not depend on the non-relativistic friction parameter $\eta_{\rm NR}$ and is equivalent to $\tilde{\mathcal{F}}(\phi_+, T_+) - \tilde{\mathcal{F}}(\phi_-, T_+) > 0$, which is the criterion provided in Ref. [10]. We wish to emphasize that Eq. (35) is just a *necessary* condition: if it is not fulfilled, then the wall cannot run away (since the total force in the runaway regime would then be negative). However, it is not a *sufficient* condition for the wall to run away, since it was obtained by assuming that the wall is already in the runaway regime. Thus, Eq. (35) implies that the runaway solution exists, but does not guarantee that it will be realized. It is well known that multiple hydrodynamical solutions may exist for the same set of parameters. Before the wall reaches ultra-relativistic velocities, the forces are not like in Eq. (34), and it may be possible for the friction to compensate the driving force. Even if the friction force is smaller for smaller velocities, hydrodynamic effects slow down the wall, acting effectively as a friction [26].

To be specific, consider a very fast detonation. In the limit in which the terminal velocity $v_w \to 1$, we have $v_\pm \to 1$. However, for a detonation, the difference of temperature between both sides of the wall does not disappear in the limit $v_w \to 1$. The friction force is

not too sensitive to temperature gradients, though, and it should be given, for $\gamma_w \gg 1$, by $F_{\rm fr}/A = \eta_{\rm UR}$. Thus, the friction for the detonation is as in Eq. (34). However, the driving force is not, since it is very sensitive to temperature gradients. Using the approximation (14), we have $F_{\rm dr}/A = p_-(T_-) - p_+(T_+) - \langle s\rangle(T_- - T_+)$. For a stationary solution, the driving force equals the friction force, and we have $F_{\rm dr}/A = \eta_{\rm UR}$. For smaller velocities, the friction is in principle smaller, and so is the driving force. Hence, for detonations, $F_{\rm dr}/A = \eta_{\rm UR}$ is the maximum value the driving force can reach. We thus have a necessary condition for the stationary solution, namely, $F_{\rm dr}/A \leq \eta_{\rm UR}$. If this condition is not satisfied, i.e., if

$$p_-(T_-) - p_+(T_+) - \langle s\rangle(T_- - T_+) > \eta_{\rm UR}, \tag{36}$$

then the stationary detonation solution does not exist.

We notice that the two conditions (35) and (36) are really different[3] since, for the detonation, the temperature T_- is always higher than T_+. If Eq. (36) is fulfilled, then the necessary condition (35) is also fulfilled. Indeed, given $\eta_{\rm UR}$ and T_+, the force $p_-(T_+) - p_+(T_+)$ is larger than $p_-(T_-) - p_+(T_+) - \langle s\rangle(T_- - T_+)$, since the latter is affected by hydrodynamics. Therefore, Eq. (36) gives a *sufficient condition* for runaway walls, corresponding to the detonation velocity becoming $v_w = 1$.

According to the above, as the parameters are varied there will exist a runaway solution before the stationary solution ceases to exist, and vice versa. Hence, the runaway and the detonation solutions will coexist in a certain range of parameters. This range is delimited by the conditions (35) and (36). Stability analysis indicate that the detonation is generally a stable solution [17]. Therefore, we expect that the wall will not runaway in the coexistence range. This range will be short if the latent heat is relatively small ($L \ll T^4$). Indeed, in such a case we will have $T_+ \simeq T_-$, and Eqs. (35) and (36) will give a similar condition.

4 Phenomenological model for the friction

In order to simplify the treatment of phase transition fronts, it is usual to replace the last term in the field equation (8), corresponding to the deviations from equilibrium, with a phenomenological damping term.

4.1 Existing models

4.1.1 "Old" phenomenological model

A widely used approximation is a damping term proportional to $u^\mu \partial_\mu \phi$. The coefficient of this term can be determined by comparing the resulting friction force (or wall velocity) with the results of microphysics calculations such as those considered in the previous

[3] According to the exact expression (13), for $T_- \neq T_+$ we could still have $F_{\rm dr}/A = p_-(T_+) - p_+(T_+)$ if $\phi(z) \equiv \phi_-$ across the wall, which is not the case.

section. In the general case, the coefficient is field-dependent,

$$\partial_\mu \partial^\mu \phi + \frac{\partial \mathcal{F}}{\partial \phi} + f(\phi)\, u^\mu \partial_\mu \phi = 0. \tag{37}$$

We shall refer to this approach as the "old" phenomenological model.

Proceeding like in the previous section, i.e., assuming a field profile of the form $\phi(z,t) = \phi[\gamma_w(z - z_w)]$, considering a reference frame which instantaneously moves with the wall, multiplying by ϕ' and integrating across the wall, we obtain

$$\sigma \ddot{z}_w = \int \frac{\partial \mathcal{F}}{\partial \phi} \frac{d\phi}{dz} dz + \int \gamma v f(\phi) (\phi')^2 dz. \tag{38}$$

where $v(z)$ is the (negative) fluid velocity and $\gamma = 1/\sqrt{1 - v^2}$. The first term in the rhs is the driving force, and the last term gives a friction force which, for small velocities, can reproduce the form (16). Indeed, for small v_w the temperature and fluid velocity are not significantly altered by the wall. Hence, the temperature is homogeneous and the fluid velocity is given by $v \approx -v_w$. We thus have

$$\sigma \ddot{z}_w = p_-(T) - p_+(T) - \eta_{\rm NR} v_w. \tag{39}$$

with

$$\eta_{\rm NR} = \int f(\phi) \phi'^2 dz \tag{40}$$

The function $f(\phi)$ can be chosen so that Eq. (40) reproduces the friction coefficient obtained from a microphysics calculation, such as Eq. (16). For the case of small m_i/T, we can choose

$$f(\phi) = \hat{\eta}_{\rm NR} \phi^2 / T, \tag{41}$$

so that we obtain the result of Eq. (18).

In the general case, hydrodynamics must be taken into account. In particular, Eqs. (4-5) imply that the fluid velocity and the temperature are in general different on each side of the wall. In sec. 3.1 we found an approximation for the first integral in Eq. (38). For the second integral, we notice that $\phi'(z)^2$ peaks inside the wall and vanishes outside. According to the weighted mean-value theorem for integrals [30], we can replace the function $f(\phi)\gamma v$ with its value at a certain point $z = \bar{z}$ inside the wall. We shall approximate this value by $f(\phi_0/2)\langle \gamma v \rangle$, with $\langle \gamma v \rangle \equiv (\gamma_- v_- + \gamma_+ v_+)/2$. With this approximation, the friction force per unit area, including hydrodynamics effects, is given by

$$\frac{F_{\rm fr}}{A} = \eta_{\rm NR} \langle \gamma v \rangle. \tag{42}$$

For the case of Eq. (41), we have $\eta_{\rm NR} = \hat{\eta}_{\rm NR} (\phi_0^2/4)\, \sigma/T$.

Although the phenomenological model (37) gives the correct form of the friction in the non-relativistic limit, for relativistic velocities the friction force (42) is of the form $F_{\rm fr}/A \sim -v_w \gamma_w$, which does not saturate in the ultra-relativistic limit. As a consequence, this model gives always stationary solutions. Even for $\eta_{\rm NR} \to 0$ we have detonation solutions and never runaway solutions.

4.1.2 A friction which saturates

Recently [15], a simple modification of the usual damping term $u^\mu \partial_\mu \phi$, was considered in order to take into account the friction saturation. In our notation, the damping term is of the form

$$\frac{f(\phi)\, u^\mu \partial_\mu \phi}{\sqrt{1 + (\lambda_\mu u^\mu)^2}}. \tag{43}$$

The constant vector λ_μ is given by $\lambda_\mu = (0, 0, 0, 1)$ in the wall frame, and the function $f(\phi)$ is given by Eq. (41), $f(\phi) = (\hat{\eta}_{\rm NR}/T)\phi^2$, so that the friction parameter can be determined by comparison with microphysics calculations in the non-relativistic regime. With the modification (43), the factor γv in Eq. (38) gets replaced by v. This gives a friction per unit area of the form

$$F_{\rm fr}/A = \eta_{\rm NR} \langle v \rangle, \tag{44}$$

which has a correct small-velocity behavior as well as Eq. (42) and, besides, saturates for large γv. More recently, in Ref. [16] the old model was considered, again with a function $f(\phi)$ of the form $f(\phi) = (\eta/T)\phi^2$, but with a velocity-dependent coefficient $\eta = \eta_0/\gamma$, so that the γ factor in Eq. (38) cancels out. The coefficient η_0 is determined by calibrating with non-relativistic results. Therefore, this approach gives again a friction of the form (44).

Although the friction (44) saturates for $v \to 1$, we note that this approximation is too simplistic, as the friction coefficient is determined in the NR limit. Numerically, this model cannot give a correct value for the friction in the UR limit, unless $\eta_{\rm UR} = \eta_{\rm NR}$. Conversely, if the coefficient in Eq. (44) were determined by $\eta_{\rm UR}$ instead of $\eta_{\rm NR}$, then the model would not give the correct value of the friction in the non-relativistic limit. Notice that $\eta_{\rm NR}$ and $\eta_{\rm UR}$ will have in general different parametric dependence, given, e.g., by Eqs. (18-19) or by Eq. (33), respectively. It is clear that a model with a single parameter falls short of describing the friction in the two opposite regimes. A more realistic interpolating model should include two free parameters.

4.2 Adding a free parameter

The vector λ_μ in the model (43) may arise as an effective value of a covariant vector. It is associated to the presence of the wall and, therefore, should depend on gradients of the field. Therefore, we propose the following phenomenological equation for ϕ,

$$\partial_\mu \partial^\mu \phi + \frac{\partial \mathcal{F}}{\partial \phi} + \frac{f(\phi)\, \partial_\mu \phi\, u^\mu}{\sqrt{1 + [g(\phi)\, \partial_\mu \phi\, u^\mu]^2}} = 0. \tag{45}$$

We have chosen a form of the damping term similar to that of Eq. (43), which will allow us to compare our results to those of Refs. [15, 16]. Notice that other forms [e.g., $u^\mu \partial_\mu \phi/(1 + \lambda_\mu u^\mu)$] reproduce as well the two behaviors $F_{\rm fr} \sim v$ and $F_{\rm fr} \sim$ constant in the NR and UR limits, respectively. Thus, in our model the phenomenological vector λ_μ

arises from derivatives of the field. In practice, the important difference with the model (43) is that the z component λ_z is not set to 1, but gives a new free parameter which can be set so as to obtain the correct UR limit.

Let us consider a reference frame which instantaneously moves with the wall (in which most time-derivatives vanish). The phenomenological damping term is given by

$$\frac{f(\phi)\,\phi'\,\gamma v}{\sqrt{1+\left[g(\phi)\,\phi'\,\gamma v\right]^2}} = 0. \tag{46}$$

The field derivative appearing in the denominator is responsible for a correct correspondence with the deviations from local equilibrium, as discussed in section 3. In the non-relativistic limit, the damping term (46) is proportional to ϕ' and, thus, is localized inside the wall. This corresponds to assuming that the departure from equilibrium occurs inside the wall. This is reasonable for a slow wall since, after the wall has passed through a given point in space, the system quickly reaches the thermodynamical equilibrium. On the other hand, in the ultra-relativistic limit ϕ' cancels out (together with γv). For $f(\phi) \propto \phi^2$ as in Eq. (41), the damping term vanishes in front of the wall but not behind it, since ϕ varies from $\phi_+ = 0$ to $\phi_- \neq 0$. This is also reasonable since, as we have seen, in the runaway regime the deviations from equilibrium occur at the wall and behind.

Proceeding as before, in the reference frame which moves with the wall we obtain

$$\sigma \ddot{z}_w = \int \frac{\partial \mathcal{F}}{\partial \phi}\frac{d\phi}{dz}dz + \int \frac{\gamma v f(\phi)(\phi')^2}{\sqrt{1+(\gamma v)^2 g(\phi)^2(\phi')^2}}dz. \tag{47}$$

The friction is given by the second integral in Eq. (47). For $v_w \ll 1$ we recover Eqs. (38-39), i.e., we obtain a linear friction force,

$$\left.\frac{F_{\rm fr}}{A}\right|_{\rm NR} = -v_w \int dz f(\phi)(\phi')^2 \equiv -\eta_{\rm NR} v_w, \tag{48}$$

whereas for $\gamma v \gg 1$ we obtain a constant friction force,

$$\left.\frac{F_{\rm fr}}{A}\right|_{\rm UR} = -\int \frac{f(\phi)}{g(\phi)}d\phi \equiv -\eta_{\rm UR}. \tag{49}$$

The functions $f(\phi)$ and $g(\phi)$ can be chosen so that Eqs. (48) and (49) give the desired values of the friction coefficients $\eta_{\rm NR}$ and $\eta_{\rm UR}$ in different models. For instance, a function $f(\phi) = \hat{\eta}_{\rm NR}\phi^2/T$ gives again a friction coefficient of the form (18) in the non-relativistic limit. With this choice for $f(\phi)$, a ϕ-independent function

$$g(\phi) = \frac{\hat{\eta}_{\rm NR}}{\hat{\eta}_{\rm UR}}\frac{1}{3T^2} \tag{50}$$

gives a friction coefficient of the form (33) in the ultra-relativistic limit. For intermediate velocities the friction depends on the velocity profile as well as on the field profile.

Solving the set of differential equations for v, T and ϕ is out of the scope of the present paper. Instead of that, we shall use the thin-wall approximation as before in order to obtain analytical results. Invoking again the weighted mean-value theorem for integrals, we notice that the friction integral in Eq. (47) can be evaluated by replacing the whole coefficient of $(\phi')^2$ with its value at a certain point $z = \bar{z}$ inside the wall[4]. It should be a good approximation to assume that $\phi'(z)$ is symmetric and, thus, picks the values $\phi = \phi_0/2$ and $\lambda_z = g(\phi_0/2)\phi'(\bar{z})$. In the thin-wall approximation one can estimate ϕ' as, e.g., $\phi' \sim \phi_0/l_w$. In fact, whatever approximation we use for ϕ', we still have the freedom to choose the function $g(\phi)$ so as to obtain the desired value of the friction parameter $\eta_{\rm UR}$. With these approximations the model essentially reduces to Eq. (43), only that in our case $\lambda_z \neq 1$. It remains to find an approximation for $v(\bar{z})$. The simplest and more reasonable one would be $v(\bar{z}) \approx \langle v \rangle \equiv (v_+ + v_-)/2$. This gives a friction force

$$\frac{F_{\rm fr}}{A} = \frac{\eta_{\rm NR}\langle v \rangle}{\sqrt{1-(1-\lambda_z^2)\langle v \rangle^2}}. \tag{51}$$

Notice that in Eq. (42) the approximation $\langle v\gamma \rangle$ was used instead of $\langle v \rangle \gamma(\langle v \rangle)$. In order to compare with previous results, in the present paper we shall use, accordingly,

$$\frac{F_{\rm fr}}{A} = \eta_{\rm NR} \left\langle \frac{v}{\sqrt{1-(1-\lambda_z^2)v^2}} \right\rangle \tag{52}$$

instead of Eq. (51), so that for $\lambda_z = 0$ we recover Eq. (42). For $\lambda_z = 1$ we recover Eq. (44). There should not be a significant difference in using either of Eqs. (51), (52).

The behavior of this friction force for different values of λ_z is shown in Fig. 1 (where the effects of hydrodynamics have been neglected, so that $v = -v_w$). The old model (37) corresponds to the case $\lambda_z = 0$ and gives a friction which never saturates. We see that, the larger the value of λ_z, the sooner the friction saturates. The models considered in Refs. [15, 16] correspond to the case $\lambda_z = 1$. This gives a friction which, in the ultra-relativistic limit, is a constant proportional to $\eta_{\rm NR}$. In the limit $v_w \to 1$, our model gives $F_{\rm fr}/A = -\eta_{\rm NR}/\lambda_z$. Comparing with Eq. (29), we see that the parameter λ_z is given by

$$\lambda_z = \frac{\eta_{\rm NR}}{\eta_{\rm UR}}, \tag{53}$$

which shows explicitly that the particular case $\lambda_z = 1$ corresponds to $\eta_{\rm UR} = \eta_{\rm NR}$, whereas the case $\lambda_z = 0$ corresponds to the limit $\eta_{\rm UR} \to \infty$. In terms of the two independent friction parameters, the equation for the wall reads

$$\sigma \ddot{z}_w = p_-(T_-) - p_+(T_+) + \langle s \rangle (T_+ - T_-) + \left\langle \frac{\eta_{\rm NR}\eta_{\rm UR} v}{\sqrt{\eta_{\rm NR}^2 v^2 + \eta_{\rm UR}^2(1-v^2)}} \right\rangle, \tag{54}$$

where we have used the approximation (14) for the driving force.

[4]Although the damping term (46) does not vanish behind the wall in the UR limit, in Eq. (47) there is an extra factor of ϕ' in the integral for the force acting on the wall.

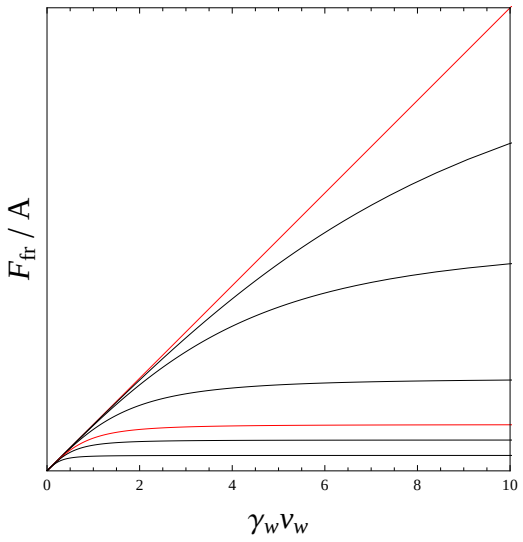

Figure 1: A friction force of the form $v_w/\sqrt{1-(1-\lambda_z^2)v_w^2}$. From top to bottom the curves correspond to $\lambda = 0, 0.1, 0.2, 0.5, 1, 1.5$ and 3. Red lines indicate the cases $\lambda = 0$ and $\lambda = 1$.

5 The wall velocity

In this section we shall study the wall velocity, considering independent variations of the friction coefficients, the nucleation temperature T_n, and other thermodynamical quantities. To proceed further, we need to consider an equation of state. It is convenient to use the well-known bag EOS, which is simple enough to obtain analytical and model independent results.

5.1 The bag EOS

The bag EOS can be derived from a free energy density of the form

$$\mathcal{F}_+(T) = -a_+ T^4/3 + \epsilon, \quad \mathcal{F}_-(T) = -a_- T^4/3. \tag{55}$$

Thus, the metastable phase is characterized by radiation and false vacuum, whereas in the stable phase we only have radiation. In this model the speed of sound is a constant, $c_\pm = 1/\sqrt{3}$. More generally, we could consider a nonvanishing vacuum energy density ϵ_- in the stable phase. For simplicity we just set $\epsilon_- = 0$ and $\epsilon_+ = \epsilon$. The only difference is that all our results below would otherwise depend[5] on $\Delta\epsilon = \epsilon_+ - \epsilon_-$ instead of ϵ. Some words are worth, though, on using these results. In a real model, ϵ_+ and ϵ_- will be given in general by the scale v of the model. Thus, we will naturally have $\epsilon_\pm \sim v^4$. In contrast, $\Delta\epsilon$ may be much smaller than that, since only a part of the false vacuum energy is in

[5]The false vacuum energy density affects the development of a phase transition through the dependence of the expansion rate of the universe on the total energy density. However, our results for the wall velocity as a function of thermodynamic and friction parameters depend only on $\Delta\epsilon$.

general released at $T = T_c$. For instance, in a second-order phase transition we will have $\Delta\epsilon = 0$. Hence, for application of our results, it must be taken into account that $\Delta\epsilon \equiv \epsilon$ corresponds to the false vacuum energy density *that is released at* $T = T_c$, and not the *total* false vacuum energy density. For that reason, it is convenient to use, instead of ϵ, the latent heat L, which in a particular model can be easily calculated as explained in section 2. Notice that L is larger than ϵ, since thermal energy is released in addition to false vacuum energy. For the bag EOS the critical temperature is given by the equation

$$(a_+ - a_-)T_c^4 = 3\epsilon, \tag{56}$$

and we have the simple relation

$$L = 4\epsilon, \tag{57}$$

since a thermal energy density $(a_+ - a_-)T_c^4$ is released in addition to the vacuum energy density ϵ.

We shall consider bubbles nucleated at a temperature $T_n < T_c$. Hydrodynamics will be dominated by the pressure difference between phases, $\Delta p \equiv p_-(T_n) - p_+(T_n)$, and by the energy density which is released at the phase transition fronts, $\Delta\rho \equiv \rho_+(T_n) - \rho_-(T_n)$. For T_n close to T_c we have $\Delta p \simeq 0$ and $\Delta\rho \simeq L$. In contrast, for $T_n \to 0$ (i.e., for strong supercooling), the pressure difference, as well as the released energy, are just given by $\Delta\rho = \Delta p = \epsilon$. As we have seen, in the general case the driving force is not just given by Δp, since it is affected by temperature gradients.

Let us first consider stationary solutions. The fluid discontinuity equations (4-5) can be used to eliminate the pressure difference $p_- - p_+$ from Eq. (54). For the bag EOS, this gives a relatively simple equation [21, 26],

$$\frac{2v_+v_-}{1-3v_+v_-} - \frac{(1+\hat{s})(1-\hat{T})}{3\alpha_+} + \frac{\eta_{\rm NR}}{L}\left[\frac{|v_+|\gamma_+}{\sqrt{1+\lambda_z^2(v_+\gamma_+)^2}} + (+\to -)\right] = 0, \tag{58}$$

where

$$\alpha_+ = \frac{\epsilon}{a_+T_+^4} = \frac{L}{4a_+T_+^4}, \tag{59}$$

$$\hat{s} \equiv \frac{s_-}{s_+} = \frac{a_-}{a_+}\hat{T}^3, \tag{60}$$

and

$$\hat{T} \equiv \frac{T_-}{T_+} = \left[\frac{a_+}{a_-}\left(1 - \frac{1+v_+v_-}{1-3v_+v_-}3\alpha_+\right)\right]^{1/4}. \tag{61}$$

In the last expression, we used again the fluid equations (4-5) to write the enthalpy ratio w_-/w_+ in terms of v_+ and v_-. Thus, Eq. (58) relates the fluid variables v_+, v_-, α_+. Besides these variables, Eq. (58) only depends on the parameter ratios $\eta_{\rm NR}/L, \eta_{\rm UR}/\eta_{\rm NR}, a_-/a_+$. The later can be written as $a_-/a_+ = 1 - 3\alpha_c$, with $\alpha_c = \epsilon/(a_+T_c^4)$. Additionally, Eqs. (4-5) give a relation between v_+ and v_- [24],

$$v_+ = \frac{1}{1+\alpha_+}\left[\frac{1}{6v_-} + \frac{v_-}{2} \pm \sqrt{\left(\frac{1}{6v_-} + \frac{v_-}{2}\right)^2 + \alpha_+^2 + \frac{2}{3}\alpha_+ - \frac{1}{3}}\right]. \tag{62}$$

The plus and minus signs in Eq. (62) indicate that we have two hydrodynamical solutions, namely, detonations and deflagrations. Using this relation, one can readily solve Eq. (58) to obtain the velocities $v_\pm$ as functions of α_+ (hence, as functions of T_+). To obtain the wall velocity as a function of the nucleation temperature T_n, appropriate boundary conditions must be used. The relation between the fluid velocities $v_\pm$ and the wall velocity v_w, as well as the relation between α_+ and $\alpha_n \equiv \epsilon/(a_+ T_n^4)$, depend on the type of hydrodynamic solution. For detonations we have simply $\alpha_+ = \alpha_n$ and $v_+ = -v_w$. For deflagrations, the matching conditions at the shock discontinuity must be used. These give

$$\frac{v_w - |v_+|}{1 - |v_+| v_w} = \frac{\sqrt{3}\,(\alpha_n - \alpha_+)}{\sqrt{(3\alpha_n + \alpha_+)\,(3\alpha_+ + \alpha_n)}}. \tag{63}$$

For traditional deflagrations we have $v_- = -v_w$, whereas for Jouguet deflagrations we have $v_- = c_s = -1/\sqrt{3}$ (for details see Refs. [21, 26]).

Using the bag EOS, we can also express the runaway conditions in terms of the thermodynamic parameters and the ultra-relativistic friction coefficient. From Eqs. (55-57), we have $p_-(T_n) - p_+(T_n) = (L/4)(1 - T_n^4/T_c^4)$, and the necessary condition (35) gives simply

$$\frac{T_n^4}{T_c^4} + \frac{\eta_{\rm UR}}{\epsilon} < 1. \tag{64}$$

We may express this condition as $\eta_{\rm UR} < \eta_{\rm nec}$, with

$$\eta_{\rm nec}/\epsilon \equiv 1 - \alpha_c/\alpha_n. \tag{65}$$

In terms of the α variables, we have

$$\alpha_n > \alpha_{\rm nec} \equiv \frac{\alpha_c}{1 - \eta_{\rm UR}/\epsilon}. \tag{66}$$

We remark that Eqs. (64-66) only give a necessary condition for the wall to run away, as the runaway solution may coexist with a detonation solution, which is presumably stable. Nevertheless, detonations are not possible if the sufficient condition (36) is fulfilled. For the bag EOS and for a detonation with $v_w \approx 1$, we have $p_-(T_-) - p_+(T_+) = L/2$, $T_-/T_+ = (a_-/a_+)^{-1/4}(1+3\alpha_n)^{1/4}$, and $s_-/s_+ = (a_-/a_+)^{1/4}(1+3\alpha_n)^{3/4}$ (for analytic approximations for ultra-relativistic detonations see Ref. [26]). We thus obtain the sufficient runaway condition $\eta_{\rm UR} < \eta_{\rm suf}$, with

$$\frac{\eta_{\rm suf}}{\epsilon} = \frac{2}{3\alpha_n}\left[(1-3\alpha_c)^{\frac{1}{4}}(1+3\alpha_n)^{\frac{3}{4}} - (1-3\alpha_c)^{-\frac{1}{4}}(1+3\alpha_n)^{\frac{1}{4}}\right]. \tag{67}$$

Equivalently, for given values of $\eta_{\rm UR}/\epsilon$ and α_c we may express this condition as $\alpha_n > \alpha_{\rm suf}$, i.e., in terms of the amount of supercooling which is sufficient for the wall to runaway. The value of $\alpha_{\rm suf}$ is obtained by inverting Eq. (67). This amounts to solving a quartic equation for the variable $x = (1+3\alpha_n)^{1/4}$. The expression for $\alpha_{\rm suf}$ is cumbersome and we shall not write it down.

Before going on to the interpretation of these results, it is worth comparing them with the previous works [15, 16]. The runaway necessary condition can be written in terms of fundamental parameters rather than phenomenological ones. Going back to the original expression $\tilde{p}_-(T_+) > p_+(T_+)$, and taking into account the fact that $\tilde{p}_-$ is given by the $\mathcal{O}(\phi^2)$ expansion of the thermal part of the effective potential, one may use the approximation (31) to write the condition as $\epsilon > T_n^2\phi_-^2 \sum c_i g_i h_i^2/24$ or, dividing by $a_+ T_n^4$, as

$$\alpha_n > \alpha_{\rm nec} \equiv \frac{30}{\pi^2}\left(\frac{\phi_-}{T_n}\right)^2 \frac{\sum c_i g_i h_i^2/24)}{\sum c_i' g_i}. \tag{68}$$

Of course, this condition is equivalent to Eq. (66), i.e., $\alpha_{\rm nec} = \alpha_c/(1-\eta_{\rm UR}/\epsilon)$. Although Eq. (68) is discussed in Ref. [15], the simple phenomenological model used for explicit calculations corresponds to setting $\eta_{\rm UR} = \eta_{\rm NR}$, which gives $\alpha_{\rm nec} = \alpha_c/(1-\eta_{\rm NR}/\epsilon)$. Similarly, in Ref. [16] the dependence of the microphysics on the wall velocity is discussed in some detail. However, when hydrodynamics is included in the calculation, a friction of the form η_0/γ is assumed. As we have already mentioned, this phenomenological model corresponds again to $\eta_{\rm UR} = \eta_{\rm NR}$.

5.2 Stationary and runaway regimes

From Eq. (64) we see that the existence of runaway solutions requires that both the UR friction parameter and the nucleation temperature be small enough. In particular, the necessary condition is never fulfilled for $\eta_{\rm UR} > \epsilon$, no matter how small T_n/T_c. This is because the pressure difference $\Delta p(T_n)$ is bounded by ϵ ($\Delta p \to \epsilon$ for $T_n \to 0$) as much as the friction is bounded by $\eta_{\rm UR}$. For $\eta_{\rm UR}$ smaller than, but close to ϵ, a strong supercooling is required [i.e., $(T_n/T_c)^4 \ll 1$]. Conversely, if the amount of supercooling is small (i.e., $T_n \approx T_c$), then $\eta_{\rm UR} \ll \epsilon$ is required. The quantity $\epsilon = L/4$ is related to the strength of the phase transition. Notice that the parameter $\alpha_c = L/(4a_+T_c^4)$ is limited to the range $0 < \alpha_c < 1/3$. The lower limit corresponds to a second-order phase transition with $a_- = a_+$ and $L = 0$. The higher limit corresponds to the case $a_- = 0$ and $L = T_c s_+(T_c)$, i.e., to maximum entropy discontinuity at $T = T_c$. Figure 2 illustrates the necessary condition (64) and the sufficient condition (67) in parameter space. In terms of $\eta_{\rm UR}/\epsilon$, the necessary condition does not depend on the parameter α_c (left panel). In terms of $\eta_{\rm UR}/(a_+T_n^4)$, it does (right panel).

In the region above the blue lines the runaway solution does not exist. Below these curves the runaway solution exists, but it may coexist with stationary solutions. The red lines indicate the limits of existence of detonation solutions. Thus, for a given value of α_c, the region above the corresponding red curve belongs to detonations or other stationary solutions, whereas the runaway solution is possible, in principle, only below the curve. Qualitatively, the two conditions have a similar behavior in the $(T_n, \eta_{\rm UR})$-plane. Both require small enough values of $\eta_{\rm UR}$ and T_n. Quantitatively, the sufficient condition is more restrictive and has a stronger dependence on hydrodynamics. This is because, for the stationary solution, the released energy causes reheating and bulk motions of the fluid.

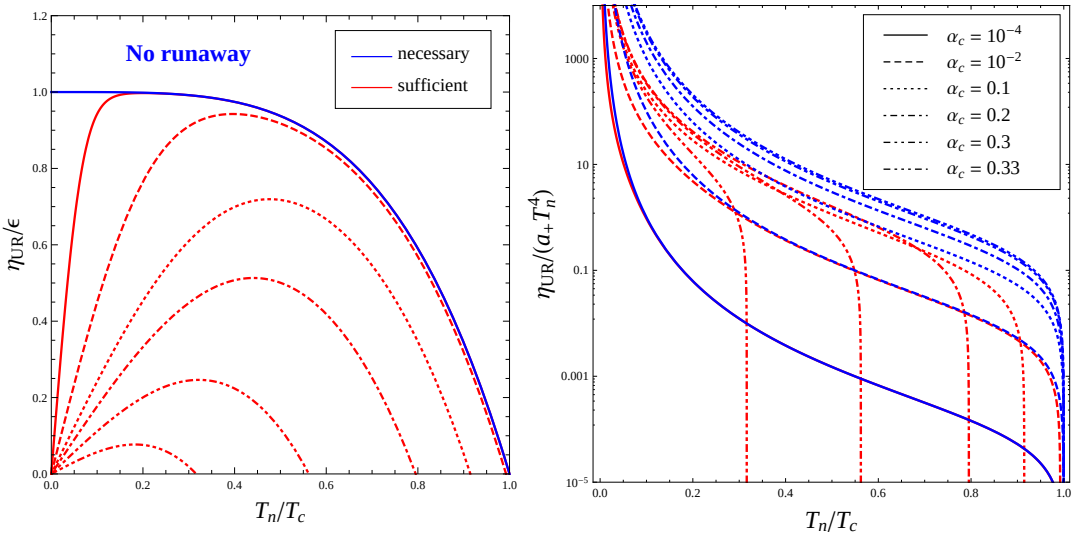

Figure 2: Regions in the $(T_n, \eta_{\rm UR})$-plane where runaway and detonation solutions can exist. The runaway necessary condition (64) is fulfilled below the blue lines. The sufficient condition (67) is fulfilled below the red lines.

The runaway wall causes less perturbations, since the released energy goes mainly into accelerating the wall.

Runaway solutions are driven by the pressure difference $\Delta p(T_n)$. For T_n close to T_c, we have $\Delta p(T_n) \approx 0$ and there won't be runaway solutions unless the friction parameter is very small, as can be seen in Fig. 2. As we increase the amount of supercooling, the pressure difference increases. For a given value of $\eta_{\rm UR}/\epsilon$, one may in principle expect that, as we keep increasing the amount of supercooling, runaway solutions will eventually be possible. As we have seen, though, the pressure difference saturates for strong supercooling (as does the friction force for high wall velocity). Thus, the wall will not run away for $\eta_{\rm UR} > \epsilon$ (see the left panel). Below the blue curve, runaway solutions become possible. However, whether the wall will run away or not, depends on the values of the parameters. Consider for instance the case $\alpha_c = 0.1$ (dotted line) and a fixed value of $\eta_{\rm UR}$. If the value of $\eta_{\rm UR}/\epsilon$ is, say, 0.8, then the wall will never run away, no matter how strong the supercooling. For a smaller friction, say, $\eta_{\rm UR}/\epsilon = 0.6$, then the wall will run away for a strong enough supercooling ($T_n/T_c \lesssim 0.66$). Eventually, for a very strong supercooling ($T_n/T_c \lesssim 0.29$) we recover again the stationary solution.

This behavior is due to the added effects of friction and hydrodynamics. Consider a weakly first-order phase transition, which is characterized by a small amount of released energy (i.e., $L \ll a_+ T_c^4$, which implies $\alpha_c \ll 1$) and a small amount of supercooling (i.e., $T_n \approx T_c$). In such a case, the effects of hydrodynamics will disappear and the sufficient condition will approach the necessary condition, as can be clearly seen in Fig. 2 (see, e.g., the cases $\alpha_c = 10^{-4}$ and $\alpha_c = 10^{-2}$). A strong phase transition is characterized by a large latent heat as well as a significant amount of supercooling. For $T_n \ll T_c$ (and $\eta_{\rm UR} < \epsilon$), one expects that the wall will run away. However, the release of latent heat slows down the

detonation, since the driving force is affected by temperature gradients. For a fixed value of the ratio $L/(a_+T_c^4)$ this effect becomes more and more important as the released energy density $\Delta\rho \sim T_c^4$ becomes large[6] in comparison with the plasma energy density $\rho \sim T_n^4$. This is why the sufficient condition departs further from the necessary condition for small T_n. The left panel of figure 2 shows that, for extremely supercooled phase transitions, the friction must be very small for the wall to run away.

In fact, microphysics gives temperature-dependent friction parameters. In a realistic model, we expect that $\eta_{\rm UR}$ will decrease at small temperatures, since the density of particles in front of the wall vanishes for $T \to 0$. Hence, the right panel in Fig. 2 may be more illustrative for small temperatures. Although the curves are more involved (since the necessary condition now depends on α_c) we see that, if we fix the value of $\eta_{\rm UR}/(a_+T_n^4)$, the system will always enter the runaway region for strong enough supercooling. We shall discuss the strong supercooling case (as well as the actual dependence of friction on temperature) in Sec. 6.

The behavior of the red curves can also be seen analytically. For $\alpha_n \sim \alpha_c \ll 1$, Eq. (67) gives $\eta_{\rm suf}/\epsilon = \eta_{\rm nec}/\epsilon - (3/8)(\alpha_c/\alpha_n)(\alpha_n + \alpha_c) + \mathcal{O}(\alpha_c^2)$. The negative sign of the $\mathcal{O}(\alpha)$ terms implies that the value $\eta_{\rm suf}$ is smaller than $\eta_{\rm nec}$. As we increase α_c, the first term in Eq. (67) decreases whereas the second term increases. Hence, the value of $\eta_{\rm suf}$ becomes smaller, departing from $\eta_{\rm nec}$. As a consequence, the region where the wall can runaway gets reduced. In the strong supercooling limit, we have a linear behavior, $\eta_{\rm suf}/\epsilon = (2/3^{1/4})(1/\alpha_c - 3)^{1/4}(T_n/T_c) + \mathcal{O}(T_n/T_c)^3$.

5.3 Stationary wall velocity

We shall now study the stationary wall velocity as a function of the parameters. We shall start the parameter variation from previously considered values [12, 13, 14, 21], which are convenient to exhibit all the kinds of hydrodynamical solutions and to compare with previous results for the old phenomenological friction model. In Fig. 3 we considered the stationary wall velocity as a function of the non-relativistic friction parameter $\eta_{\rm NR}$. Although we can vary independently $\eta_{\rm NR}$ and $\eta_{\rm UR}$, in a real model there will be some correlation between these parameters (e.g., both increase with the couplings of particles to the Higgs). Therefore, we considered two opposite relations for them. In the upper panels of Fig. 3 we fixed the ratio $\lambda_z = \eta_{\rm NR}/\eta_{\rm UR}$, whereas in the lower panels we fixed $\eta_{\rm UR}$. The left panels show all the stationary solutions for a given set of parameters. The right panel shows the solutions which are actually realized in the phase transition.

Consider first the case of fixed λ_z (upper panels). In the left panel we see that, in some cases, there are several possible solutions. In the first place, detonations and "traditional" deflagrations are bivalued in a certain range. This is not a problem, since the lower branch of detonations and the upper branch of deflagrations are unphysical solutions [26] which, according to numerical calculations, are unstable [12, 13, 14] and, thus, must be discarded[7]. On the other hand, we see that also different types of hydrodynamical

[6]For the bag model, the released energy density is bounded below by $\epsilon = L/4$.

[7]Notice that this eliminates the Jouguet detonation (corresponding to the lower endpoint of the

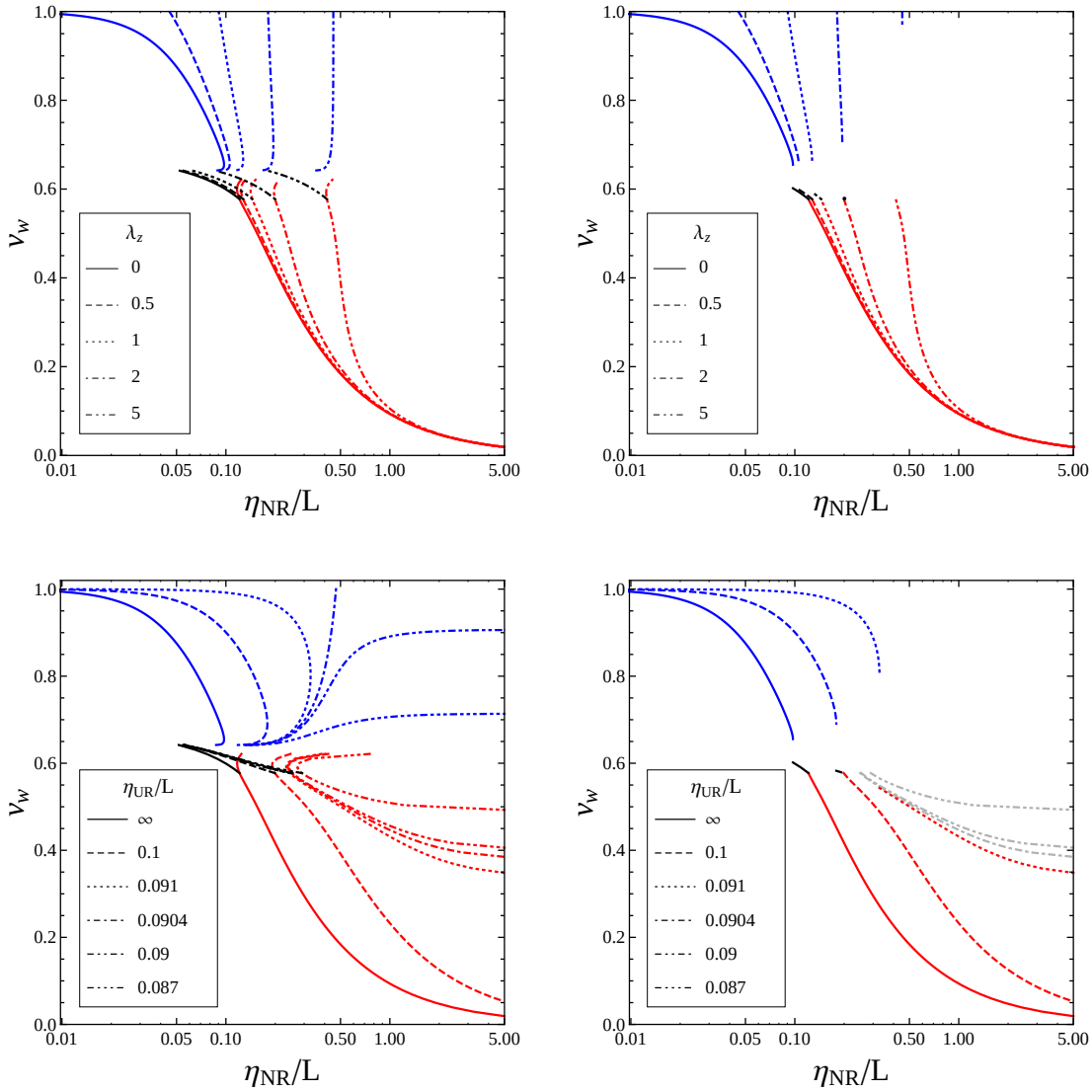

Figure 3: The wall velocity for the bag model with $\alpha_c = 4.45 \times 10^{-3}$ and $T_n = 0.89T_c$. Detonations are in blue, "traditional" deflagrations are in red, and Jouguet deflagrations are in black. The right panels show only the stable solutions.

solutions may coexist. Numerical calculations seem to indicate that supersonic traditional deflagrations, which are strong deflagrations, are unstable. Thus, the only supersonic deflagration which can be realized is the Jouguet deflagration. In case of coexistence of a deflagration with a detonation, the detonation seems to be the stable solution [12, 13, 14]. We have plotted the curves in the right panel assuming this hierarchy.

The case $\lambda_z = 0$ (solid line) corresponds to the widely used model (37), which does not exhibit runaway behavior. For $\lambda_z \neq 0$ the friction (52) saturates at high velocities and the wall may run away. The runaway behavior depends only on $\eta_{\rm UR}$. However, for fixed $\lambda_z = \eta_{\rm NR}/\eta_{\rm UR}$, the wall always runs away for small enough $\eta_{\rm NR}$, i.e., the wall velocity becomes $v_w = 1$ at $\eta_{\rm NR} = \eta_{\rm suf}/\lambda_z$ (indicating that the stationary wall assumption breaks down). Notice that the behavior is qualitatively similar for the different values of λ_z. Quantitatively, the differences become significant only for small $\eta_{\rm NR}$ or large λ_z. The particular case $\lambda_z = 1$ corresponds to the models of Refs. [15, 16], for which the friction coefficient has the same value in the two opposite regimes. Lower values of λ_z, corresponding to higher values of the UR friction, yield a wider range of parameters with stationary solutions.

In the lower panels of Fig. 3 we considered fixed values of $\eta_{\rm UR}$. We have chosen most values around $\eta_{\rm UR} = \eta_{\rm suf} \simeq 0.0904$ (dashed-dotted line). For higher values of $\eta_{\rm UR}$ the curves accumulate near the limiting line of $\eta_{\rm UR} \to \infty$ (which is the same as the curve of $\lambda_z = 0$ in the upper figure). For $\eta_{\rm UR} \leq \eta_{\rm suf}$ the detonation solutions disappear (the curves in the left panel correspond to the unphysical branches of the solutions, for which the velocity increases with the friction), and the deflagrations approach the speed of sound. The right panel shows only the physical stationary solutions. It is interesting that for $\eta_{\rm UR} \leq \eta_{\rm suf}$ there are still deflagration solutions. We show these curves in grey. However, these fast deflagrations coexist with the runaway solution, and it is possible that they are unstable[8]. Consequently, we shall assume that for $\eta_{\rm UR} < \eta_{\rm suf}$ the wall runs away. For $\eta_{\rm UR} > \eta_{\rm suf}$, we notice that there is always a physical stationary solution, no matter how small the value of the NR friction coefficient. This behavior contrasts with the upper panel, where the wall always runs away for small enough $\eta_{\rm NR}$. As we have already mentioned, in a physical model there will always be a correlation between $\eta_{\rm NR}$ and $\eta_{\rm UR}$. We do not expect, in general, a very small $\eta_{\rm NR}$ together with a considerably large $\eta_{\rm UR}$ or vice versa. As the fundamental parameters of a model are varied, we expect an intermediate behavior between the curves of the upper and lower panels.

In Fig. 4 we fixed $\eta_{\rm NR}$ and varied $\eta_{\rm UR}$. Notice that the wall velocity changes quickly near the critical value $\eta_{\rm UR} = \eta_{\rm suf}$. For larger values the velocity is essentially a constant which depends on the value of $\eta_{\rm NR}$. As $\eta_{\rm UR}$ approaches $\eta_{\rm suf}$ from the right, the velocity grows and the detonation solutions disappear (their velocity becomes $v_w = 1$). Again, we see that for $\eta_{\rm UR} < \eta_{\rm suf}$ we may still have physical deflagration solutions (in gray in

detonation curves), which has often been considered for gravitational wave generation.

[8]In general, the traditional deflagration seems to become unstable when it coexists with other stationary solutions (namely, Jouguet deflagrations or detonations). It is probable that the same happens when it coexists with the runaway solution. A stability analysis is out of the scope of this paper and shall be addressed elsewhere.

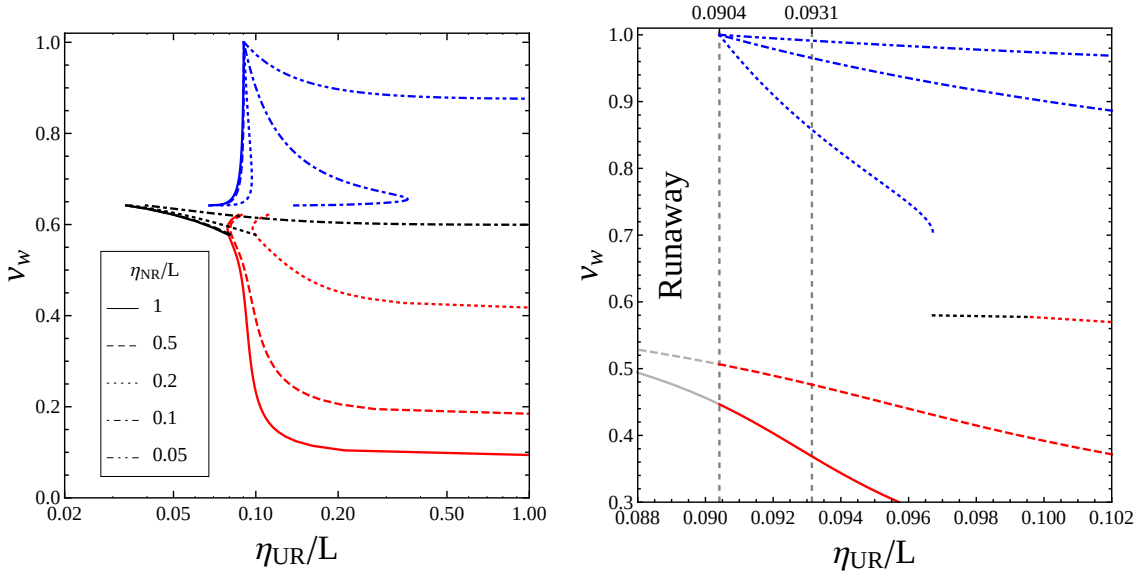

Figure 4: The wall velocity as a function of $\eta_{\rm UR}$, for the same bag parameters of Fig. 3 and several values of $\eta_{\rm NR}$. The vertical lines indicate the values of $\eta_{\rm suf}$ and $\eta_{\rm nec}$.

the right panel). As explained above, we shall assume that these are unstable and we shall chose the runaway solution. In the right panel we have zoomed the friction near $\eta_{\rm UR} = \eta_{\rm suf}$ and we have marked the values of $\eta_{\rm suf}$ and $\eta_{\rm nec}$ (which are very close to each other for the present values of α_c and α_n).

Finally, in Fig. 5 we fixed the friction parameters and varied the amount of supercooling. In the left panel we also show the speed of sound and the Jouguet detonation velocity $v_J^{\rm det}(\alpha_n)$ (dotted grey lines). We see that, for T_n close to T_c, the solution is always a weak deflagration and does not depend on the UR friction parameter. The detonation solutions reach the speed of light at $\alpha_n = \alpha_{\rm suf}$, indicating that beyond that value the wall runs away. The runaway solutions exist already from $\alpha_n = \alpha_{\rm nec}$, indicated in the right panel by black round dots on the curves. For the smallest values of λ_z (highest values of $\eta_{\rm UR}$) the velocity grows very slowly with the amount of supercooling. As we have discussed earlier, the wall may eventually decrease for strong supercooling, due to hydrodynamics effects. We shall analyze this possibility in the next section. For high values of λ_z, the ranges of stationary solutions get reduced (see the right panel). This is also observed in the previous figures. For the case $\lambda_z = 2$, the Jouguet deflagration has disappeared (the weak deflagration turns directly into a detonation) and the detonation has a very short parameter range of existence. For $\lambda_z = 5$ the detonation has also disappeared and the weak deflagration turns directly into a runaway solution at $\alpha_n = \alpha_{\rm suf}$ (we have marked this value with a squared blue dot, and we have plotted the deflagration solution in grey beyond it). As can be seen in the left panel, in this case it is the unphysical branch of detonations that reaches the speed of light.

In all these figures, we see that the detonation velocity becomes $v_w = 1$ at the values $\alpha_{\rm suf}$ or $\eta_{\rm suf}$ obtained in sec. 5.1. As we have just seen, in some cases this actually

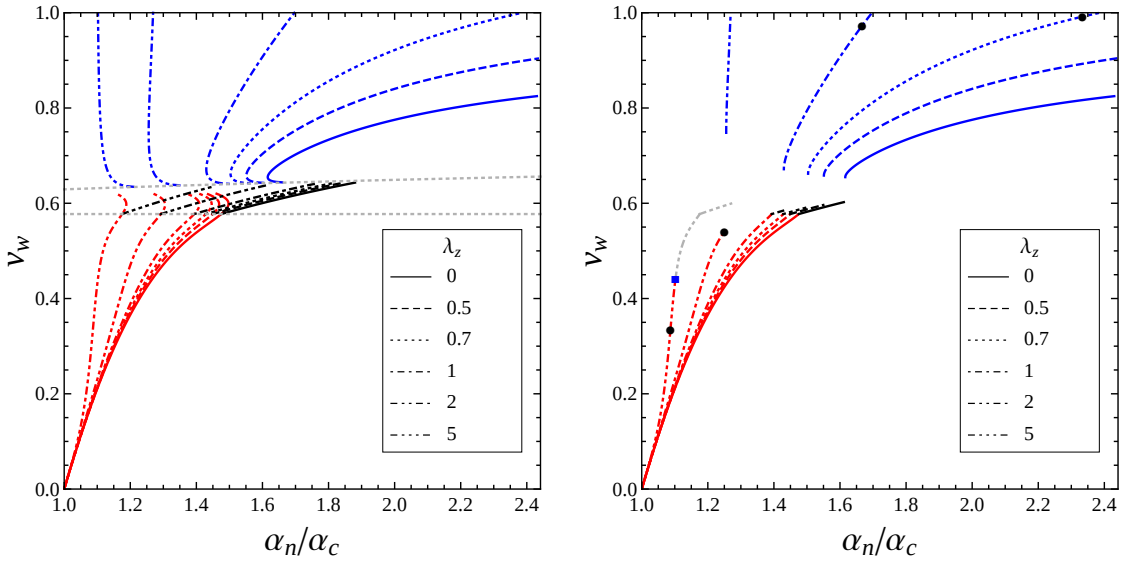

Figure 5: The wall velocity as a function of $\alpha_n/\alpha_c = (T_c/T_n)^4$, for $\alpha_c = 4.45 \times 10^{-3}$, $\eta_{\rm NR}/L = 0.1$, and several values of λ_z.

corresponds to an unphysical detonation. In general, cases like that of $\lambda_z = 5$ in Fig. 5, where the physical detonation does not exist at all, deflagrations do exist. Assuming, as we did, that in this case the deflagration becomes unstable and jumps to a runaway solution at $\alpha_n = \alpha_{\rm suf}$ (or $\eta_{\rm UR} = \eta_{\rm suf}$ in the right panel of Fig. 4), the values of $\alpha_{\rm suf}$ and $\eta_{\rm suf}$ still make sense as limits between a stationary solution (either a detonation or a deflagration) to a runaway solution. This is the actual meaning of the red curves in Fig. 2.

6 Strong supercooling

The fast propagating modes of a phase transition front, namely, detonations and runaway walls, are interesting due to the possibility of generating sizeable gravitational waves. The high velocity behavior is governed by the UR friction parameter. As we have seen, though, whether the wall will be fast or not, depends also on the amount of supercooling and on the latent heat. A considerable amount of supercooling favors large pressure differences and high velocities, whereas a large release of latent heat slows down the wall. Strong supercooling is typical of strongly first-order phase transitions. However, the latter are also characterized by a large latent heat. On the other hand, at low temperatures one expects a small friction.

The friction depends strongly on the values of the particle masses inside the bubble (assuming for simplicity that $m_i = 0$ outside); more precisely, on the ratio m_i/T. Thus, a relevant parameter is the value of ϕ/T in the broken-symmetry phase. Strongly first-order phase transitions are characterized by a relatively high value of the ratio $\phi_0(T_c)/T_c$.

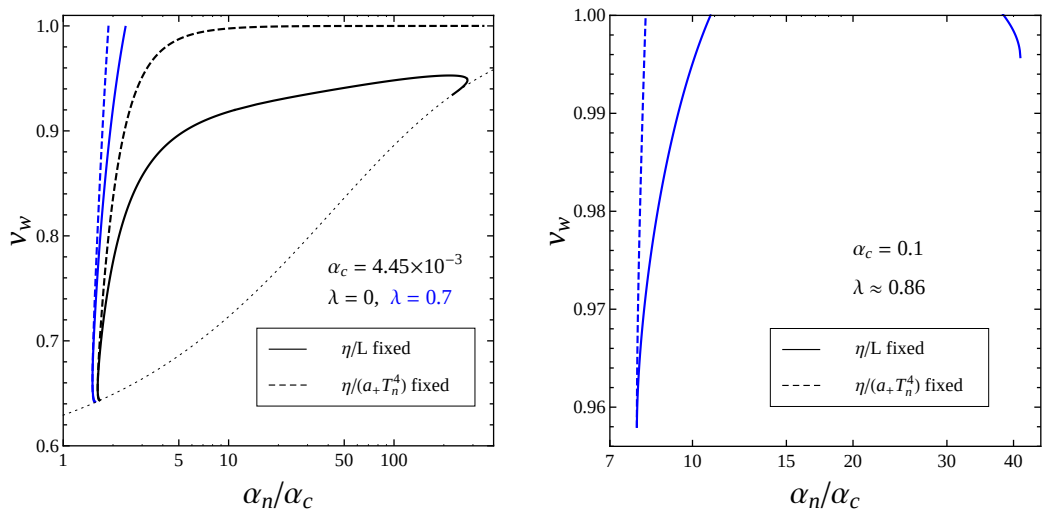

Figure 6: The wall velocity as a function of α_n/α_c for η/L fixed (solid) and $\eta/(a_+T_n^4)$ fixed (dashed). In the left panel we have $\eta_{\rm NR} = 0.1L$ for T_n close to T_c. In the right panel we have $\eta_{\rm NR} = 0.15L$ and $\eta_{\rm UR} = 0.175L$ for T_n close to T_c.

This implies also a relatively high latent heat. Nevertheless, ϕ_0 and T_c are both given by the characteristic scale of the theory, and its ratio will be $\mathcal{O}(1)$ for a natural phase transition. As we have seen, for the bag EOS, L is bounded by $\frac{4}{3}a_+T_c^4$. On the other hand, in some models the barrier between minima may persist at low temperatures, causing a large amount of supercooling. In such a case we may have $T_n \ll T_c$, which implies $\phi_0(T_n)/T_n \gg 1$ and $L \gg a_+T_n^4$.

On the whole, for very strong supercooling we will have in principle a high pressure difference between phases and a small friction force, but the energy released will be large in comparison to the energy density of the plasma, and hydrodynamics effects will be important. It is thus worth investigating the behavior of phase transition fronts in such a case.

6.1 Detonations and runaway solutions

As we have seen, strong hydrodynamics effects may prevent the wall from reaching ultra-relativistic velocities, even in the case of a strong supercooling. To illustrate this effect, let us plot again v_w vs. α_n like in Fig. 5, this time for a wider range of the supercooling parameter α_n/α_c. It is interesting to consider first the same thermodynamic parameters of Fig. 5, which correspond to a relatively low value of the released energy (since $L \sim 10^{-2}a_+T_c^4$). In the left panel of Fig. 6 we consider a couple of representative values of λ_z. As an example of the case $\eta_{\rm UR} > \epsilon$, for which the wall will not run away, we choose $\lambda_z = 0$, i.e., the limit $\eta_{\rm UR} \to \infty$ (black lines). We see that, for fixed values of the friction parameters (solid black line), the velocity grows slowly with the amount of supercooling, and eventually decreases for very strong supercooling. Moreover, for

$\alpha_n/\alpha_c \gtrsim 300$ the stationary solution cannot exist due to strong hydrodynamics effects. Before disappearing, the detonation approaches the Jouguet point (dotted grey line) and a non-physical branch of solutions appears, just like at the other end of the curve (where the supercooling becomes insufficient for a detonation solution). As we have mentioned, for strong supercooling it is more realistic[9] to consider a friction which decreases as T_n decreases. Therefore, we have also considered fixed values of $\eta/(a_+ T_n^4)$ (dashed black line). In this case, the wall velocity is only bounded by the relativistic limit $v_w = 1$. The wall does not runaway because we are considering the case $\eta_{\rm UR} \to \infty$. We also consider the case $\lambda_z = 0.7$ (blue lines). The solid line (η/L fixed) corresponds to the dotted line in Fig. 5, which runs away for $\alpha_n/\alpha_c \simeq 2.4$. For $\eta/(a_+ T_n^4)$ fixed (dashed blue line) the wall runs away at a smaller α_n.

Hydrodynamics effects will be stronger for higher values of the latent heat. In Sec. 5.2 we have discussed the case $\alpha_c = 0.1$, corresponding to the dotted line in Fig. 2. According to that figure (see the left panel), for $\eta_{\rm UR}/L \approx 0.15$ (i.e., $\eta_{\rm UR}/\epsilon \approx 0.6$) the detonation solution gives way to the runaway solution at a given amount of supercooling. But then, for a stronger amount of supercooling, the detonation solution is possible again. The right panel of Fig. 6 shows this effect (we have only kept the physical solutions and we have chosen the values $\eta_{\rm NR}/L = 0.15$ and $\eta_{\rm UR}/L = 0.175$, which better illustrate the effect). It is important to notice, however, that shortly after reappearing, the detonation ceases to exist due to strong hydrodynamics. In many cases, the detonation will not reappear at all. In any case, if we consider a friction which vanishes at zero temperature (dashed line), then a smaller supercooling will suffice for the wall to run away, and the stationary solution will not appear again at stronger supercooling. This can be seen already in the right panel of Fig. 2.

So far we have considered two simple cases for the variation of the friction coefficients with temperature, which consist of fixing the dimensionless ratios η/L and $\eta/(a_+ T_n^4)$. In a realistic model, we expect temperature-dependent friction parameters, although not necessarily decreasing as fast as T^4. Roughly, the number density of massless particles in the symmetric phase goes as T^3, and the force each particle feels at the wall is proportional to $\Delta p \approx (m/p)\Delta m$ (in the WKB approximation). For $\Delta m = m(\phi_0)$, we have $\Delta p \sim m^2/T$. Thus we obtain a force of the form $F \sim m^2 T^2$. As we shall see, this is parametrically correct for $\eta_{\rm UR}$. The case of $\eta_{\rm NR}$ is more complex because one must take into account particle interactions. For interaction rates $\Gamma \sim T$, one obtains again $F_{\rm fr} \propto T^2$ (see below).

To investigate the behavior of the wall velocity with a friction which depends quadratically on temperature, we shall consider friction parameters of the form $\eta = \eta_0 T_n^2 = \eta_0' \sqrt{\alpha_c/\alpha_n}$. We choose the coefficient η_0 so that the different forms of the friction match for $T_n \sim T_c$. In order to evaluate to what extent fast solutions depend on the NR friction parameter, we shall also consider the case of a constant $\eta_{\rm NR}$ with a quadratic $\eta_{\rm UR}$. We show the result in Fig. 7, together with the curves of Fig. 6 for comparison. The black lines correspond to both friction coefficients of the form $\eta = \eta_0 T^2$. The red lines correspond to a constant NR friction coefficient. We see that the black and red curves

[9] We discuss this issue below.

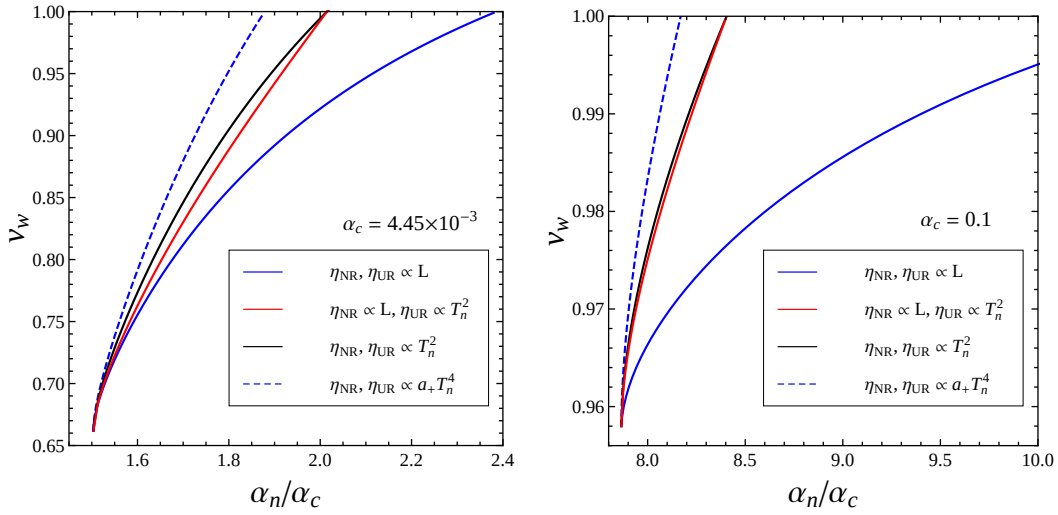

Figure 7: The same as Fig. 6 (blue lines), but we have included the cases $\eta_{\rm NR}, \eta_{\rm UR} \propto T_n^2$ (black lines) and $\eta_{\rm UR} \propto T_n^2$, $\eta_{\rm NR} =$ constant (red lines).

are very close to each other, and meet in the limit $v_w = 1$. This is because the value of the NR friction coefficient does not play a relevant role for detonations, and becomes irrelevant in the ultra-relativistic limit. In the right panel the effects of hydrodynamics are stronger since the released energy is larger (notice the larger amounts of supercooling needed to obtain detonations and runaway walls). We see that the solid line deviates significantly from the others. This corresponds to the unrealistic case in which the UR friction is temperature-independent.

6.2 Strong supercooling and friction coefficients

In this last subsection we wish to discuss briefly the behavior of the friction coefficients at low nucleation temperatures (see [28] for other limiting cases). A detailed analysis is out of the scope of the present paper. Therefore, we shall assume that the WKB approximation is still valid. For very low temperatures, such that $T \ll l_w^{-1}$ this approximation will certainly break down.

Let us first consider the non-relativistic friction coefficient $\eta_{\rm NR}$. Since the interaction rates are proportional to temperature, at low temperatures the approximation $\Gamma \gg l_w^{-1}$ which leads to Eq. (16) is no longer valid. Nevertheless, we shall consider the approximation (16) to catch a glimpse of the behavior of the friction. In any case, we have just seen that the wall velocity depends very weakly on $\eta_{\rm NR}$ for strong supercooling. In the limit $m/T \gg 1$ the coefficient c_1 is suppressed by a Boltzmann factor,

$$c_1 \approx (m/T)^{1/2} \exp\left(-m/T\right) / \left(2\pi\right)^{3/2} . \tag{69}$$

However, in the case of interest, very light particles in the symmetric phase become heavy in the broken-symmetry phase. For simplicity, let us consider masses of the form

$m_i(\phi) = h_i\phi$. To calculate the integral in Eq. (16), we notice that for small ϕ the integrand is suppressed by powers of ϕ. Therefore we can use the approximation (69) in all the range of integration. We have

$$\eta_{\rm NR} = \sum_i \frac{g_i T^4}{\Gamma(2\pi)^3} \int_0^{h\phi_0/T} e^{-2x} x^3 \left|\frac{dx}{dz}\right| dx, \tag{70}$$

with $x = h_i\phi/T$. To perform the integral, an approximation for $\phi(z)$ is needed. Instead of the usual $(\phi_0/2)([1+\tanh(z/l_w)]$, we shall use the much simpler approximation of a linear function $\phi = \phi_0/l_w\, z$ inside the wall and $\phi =$ constant outside the wall. The temperature dependence, as well as the parametric behavior, should not depend on the approximation for the wall profile. Thus, in the integral (70) dx/dz is a constant and we obtain, for $h\phi_0/T \gg 1$,

$$\eta_{\rm NR} = \sum_i \frac{3 g_i h_i \phi_0 T^2}{64\pi^3(\Gamma/T) l_w}. \tag{71}$$

We see that the friction coefficient vanishes for small T, though not as fast as T^4.

The ultra-relativistic friction coefficient is very easy to estimate in the strong supercooling limit, either from its definition in Eqs (28-29) or directly from the total force (20). It is interesting to consider the latter. For $\phi_+ = 0$ and $m_i = h_i\phi$, the total force is given, *at any temperature*, by

$$\frac{F}{A} = V(\phi_+) - V(\phi_-) - \sum_i g_i c_i h_i^2 \frac{\phi_o^2 T^2}{24}. \tag{72}$$

At high temperatures, the last term in Eq. (72) is part of the equilibrium pressure difference [as can be seen in the high-temperature expansion (31)]. Hence, it is part of the driving force. As a consequence, the friction is given by the rest of the high-T expansion, $\eta_{\rm UR} \sim T\phi_0^3 + \mathcal{O}(\phi_0^4)$ [see Eq. (33)]. At very low temperatures, on the contrary, the driving force is just given by the vacuum potential, i.e., the first two terms in Eq. (72). Hence, the last term now gives the friction force, and we have

$$\eta_{\rm UR} = \sum_i g_i c_i h_i^2 \frac{\phi_o^2 T^2}{24}. \tag{73}$$

We see that $\eta_{\rm UR}$ goes as T^2 at low temperatures.

7 Conclusions

In this paper we have studied the friction force acting on phase transition fronts. In particular, we have discussed the ultra-relativistic behavior of the friction, derived in Ref. [10]. We have considered runaway walls as well as stationary walls (detonations), which have different hydrodynamics. We have shown that the two solutions coexist in a range of parameters. Thus, we have argued that the runaway condition given in Ref. [10] is only

a necessary condition and does not guarantee that the wall will run away. We have found a sufficient condition for the wall to run away by using the criterion of the detonation reaching the speed of light.

We have also proposed a phenomenological model for the friction, which interpolates between the non-relativistic and the ultra-relativistic behaviors. The main improvement of this model with respect to previous ones is the incorporation of a new free parameter governing the ultra-relativistic limit of the friction force. The value of this parameter can be easily calculated for any specific model. Therefore, our model not only gives a saturating friction, but also gives the correct quantitative behavior of the friction in the UR limit. This phenomenological model is consistent with the necessary and sufficient runaway conditions, which do not depend on the non-relativistic friction coefficient.

Using the bag equation of state and our phenomenological model for the friction, we have studied the runaway conditions, as well as the stationary regime, as functions of the thermodynamic and friction parameters. Regarding the runaway conditions, the general result is that they are quantitatively similar for small values of the latent heat but depart otherwise. If we, for instance, increase the amount of supercooling (for a given value of the friction), then, in the case of small latent heat, the sufficient condition is reached shortly after the necessary condition. On the contrary, for larger latent heat, the larger release of energy slows down the phase transition fronts. This causes the detonation to persist for larger amounts of supercooling, even if the runaway solution already exists. Regarding the stationary wall velocity, we have found, as expected, that for parameters which favor a small wall velocity (i.e., for low supercooling, large latent heat, or high non-relativistic friction) the solution depends very weakly on the UR friction coefficient. Conversely, for parameters which favor fast stationary solutions, the velocity does not depend significantly on the NR friction coefficient.

We have studied in particular the case of a phase transition with a large amount of supercooling, which is important for the generation of gravitational waves. In this case the dependence of the friction on temperature becomes relevant. We have explored the wall velocity for different behaviors of the friction coefficients. Thus, we have considered fixed values of the dimensionless parameters η/L and η/T^4, as well as the quadratic dependence $\eta \propto T^2$. The latter is motivated by low-temperature approximations, which we have also discussed. The value of the NR friction parameter does not affect the strong supercooling case, since the velocity is in general high. The general result is that, if the UR friction parameter does not decrease for strong supercooling, then the wall may reach a saturation value, and even decrease due to hydrodynamics effects. In contrast, if the UR friction parameter vanishes at zero temperature (which seems to be the actual case), then the wall always runs away for strong enough supercooling.

Acknowledgements

This work was supported by Universidad Nacional de Mar del Plata, Argentina, grant EXA 607/12.

References

[1] For reviews, see A. G. Cohen, D. B. Kaplan and A. E. Nelson, Ann. Rev. Nucl. Part. Sci. **43**, 27 (1993) [arXiv:hep-ph/9302210]; A. Riotto and M. Trodden, Ann. Rev. Nucl. Part. Sci. **49**, 35 (1999) [arXiv:hep-ph/9901362]; T. Konstandin, arXiv:1302.6713 [hep-ph].

[2] For a review, see D. Grasso and H. R. Rubinstein, Phys. Rept. **348**, 163 (2001) [arXiv:astro-ph/0009061].

[3] A. Vilenkin and E.P.S. Shellard, *Cosmic Strings and Other Topological Defects* (Cambridge University Press, Cambridge, England, 1994); A. Vilenkin, Phys. Rept. **121**, 263 (1985).

[4] E. Witten, Phys. Rev. D **30**, 272 (1984); G. M. Fuller, G. J. Mathews and C. R. Alcock, Phys. Rev. D **37**, 1380 (1988); J. H. Applegate and C. J. Hogan, Phys. Rev. D **31**, 3037 (1985); H. Kurki-Suonio, Phys. Rev. D **37**, 2104 (1988); J. Ignatius, K. Kajantie, H. Kurki-Suonio and M. Laine, Phys. Rev. D **50**, 3738 (1994) [arXiv:hep-ph/9405336]; A. Mégevand and F. Astorga, Phys. Rev. D **71**, 023502 (2005).

[5] A. F. Heckler, Phys. Rev. D **51** 405, (1995) [arXiv:astro-ph/9407064];

[6] A. Kosowsky and M. S. Turner, Phys. Rev. D **47**, 4372 (1993); M. Kamionkowski, A. Kosowsky and M. S. Turner, Phys. Rev. D **49**, 2837 (1994); A. Kosowsky, A. Mack and T. Kahniashvili, Phys. Rev. D **66**, 024030 (2002); A. D. Dolgov, D. Grasso and A. Nicolis, Phys. Rev. D **66**, 103505 (2002); C. Caprini and R. Durrer, Phys. Rev. D **74**, 063521 (2006); C. Caprini, R. Durrer and G. Servant, Phys. Rev. D **77**, 124015 (2008) [arXiv:0711.2593 [astro-ph]]; R. Apreda, M. Maggiore, A. Nicolis and A. Riotto, Nucl. Phys. B **631**, 342 (2002); A. Nicolis, Class. Quant. Grav. **21**, L27 (2004); C. Grojean and G. Servant, Phys. Rev. D **75**, 043507 (2007); S. J. Huber and T. Konstandin, JCAP **0809**, 022 (2008) [arXiv:0806.1828 [hep-ph]]; S. J. Huber and T. Konstandin, JCAP **0805**, 017 (2008) [arXiv:0709.2091 [hep-ph]]. A. Megevand, Phys. Rev. D **78** (2008) 084003 [arXiv:0804.0391 [astro-ph]]; J. Kehayias and S. Profumo, JCAP **1003**, 003 (2010) [arXiv:0911.0687 [hep-ph]]; L. Leitao, A. Megevand and A. D. Sanchez, JCAP **1210**, 024 (2012) [arXiv:1205.3070 [astro-ph.CO]].

[7] B. H. Liu, L. D. McLerran and N. Turok, Phys. Rev. D **46**, 2668 (1992); N. Turok, Phys. Rev. Lett. **68**, 1803 (1992); M. Dine, R. G. Leigh, P. Y. Huet, A. D. Linde and D. A. Linde, Phys. Rev. D **46**, 550 (1992) [arXiv:hep-ph/9203203]; S. Y. Khlebnikov, Phys. Rev. D **46**, 3223 (1992); P. Arnold, Phys. Rev. D **48**, 1539 (1993) [arXiv:hep-ph/9302258]; G. D. Moore and T. Prokopec, Phys. Rev. D **52**, 7182 (1995) [arXiv:hep-ph/9506475]; Phys. Rev. Lett. **75**, 777 (1995) [arXiv:hep-ph/9503296]; G. D. Moore and N. Turok, Phys. Rev. D **55**, 6538 (1997) [arXiv:hep-ph/9608350].

[8] P. John and M. G. Schmidt, Nucl. Phys. B **598**, 291 (2001) [Erratum-ibid. B **648**, 449 (2003)].

[9] G. D. Moore, JHEP **0003**, 006 (2000);

[10] D. Bodeker and G. D. Moore, JCAP **0905**, 009 (2009) [arXiv:0903.4099 [hep-ph]].

[11] M. Gyulassy, K. Kajantie, H. Kurki-Suonio and L. D. McLerran, Nucl. Phys. B **237**, 477 (1984); K. Enqvist, J. Ignatius, K. Kajantie and K. Rummukainen, Phys. Rev. D **45**, 3415 (1992); H. Kurki-Suonio, Nucl. Phys. B **255**, 231 (1985); K. Kajantie and H. Kurki-Suonio, Phys. Rev. D **34**, 1719 (1986);

[12] J. Ignatius, K. Kajantie, H. Kurki-Suonio and M. Laine, Phys. Rev. D **49**, 3854 (1994);

[13] H. Kurki-Suonio and M. Laine, Phys. Rev. D **51**, 5431 (1995) [arXiv:hep-ph/9501216];

[14] H. Kurki-Suonio and M. Laine, Phys. Rev. D **54**, 7163 (1996) [hep-ph/9512202].

[15] J. R. Espinosa, T. Konstandin, J. M. No and G. Servant, JCAP **1006**, 028 (2010) [arXiv:1004.4187 [hep-ph]];

[16] S. J. Huber and M. Sopena, arXiv:1302.1044 [hep-ph].

[17] B. Link, Phys. Rev. Lett. **68**, 2425 (1992); K. Kajantie, Phys. Lett. B **285**, 331 (1992); M. Kamionkowski and K. Freese, Phys. Rev. Lett. **69**, 2743 (1992) [arXiv:hep-ph/9208202]; P. Y. Huet, K. Kajantie, R. G. Leigh, B. H. Liu and L. D. McLerran, Phys. Rev. D **48**, 2477 (1993) [arXiv:hep-ph/9212224].

[18] M. Quiros, arXiv:hep-ph/9901312.

[19] S. R. Coleman, Phys. Rev. D **15**, 2929 (1977) [Erratum-ibid. D **16**, 1248 (1977)]; C. G. Callan and S. R. Coleman, Phys. Rev. D **16**, 1762 (1977); I. Affleck, Phys. Rev. Lett. **46**, 388 (1981); A. D. Linde, Nucl. Phys. B **216**, 421 (1983) [Erratum-ibid. B **223**, 544 (1983)]; Phys. Lett. B **100**, 37 (1981).

[20] A. H. Guth and E. J. Weinberg, Phys. Rev. D **23**, 876 (1981); G. W. Anderson and L. J. Hall, Phys. Rev. D **45**, 2685 (1992); A. Megevand, Int. J. Mod. Phys. D **9**, 733 (2000) [hep-ph/0006177]; A. Megevand, Phys. Rev. D **64**, 027303 (2001) [hep-ph/0011019]; A. Megevand and A. D. Sanchez, Phys. Rev. D **77**, 063519 (2008) [arXiv:0712.1031 [hep-ph]].

[21] A. Megevand and A. D. Sanchez, Nucl. Phys. B **865**, 217 (2012) [arXiv:1206.2339 [astro-ph.CO]].

[22] L. Leitao and A. Megevand, Nucl. Phys. B **844**, 450 (2011) [arXiv:1010.2134 [astro-ph.CO]].

[23] L. D. Landau and E. M. Lifshitz, *Fluid Mechanics* (Pergamon Press, New York, 1989); R. Courant and K. O. Friedrichs, *Supersonic Flow and Shock Waves* (Springer-Verlag, Berlin, 1985).

[24] P. J. Steinhardt, Phys. Rev. D **25**, 2074 (1982).

[25] A. Megevand, Phys. Rev. D **69**, 103521 (2004).

[26] A. Megevand and A. D. Sanchez, Nucl. Phys. B **820**, 47 (2009) [arXiv:0904.1753 [hep-ph]].

[27] T. Konstandin and J. M. No, JCAP **1102**, 008 (2011) [arXiv:1011.3735 [hep-ph]].

[28] A. Megevand and A. D. Sanchez, Nucl. Phys. B **825**, 151 (2010) [arXiv:0908.3663 [hep-ph]].

[29] S. J. Huber and M. Sopena, Phys. Rev. D **85**, 103507 (2012) [arXiv:1112.1888 [hep-ph]].

[30] T. M. Apostol, *Calculus*, Vol. I, (John Wiley & Sons, New York, 1967).